Expectation and Confusion: Evidence and Theory*

HENG CHEN
University of Hong Kong
YICHENG LIU
University of Hong Kong

January 17, 2026

Abstract. In this paper, we characterize a forecasting model where forecasters cannot perfectly distinguish between the two persistent components (trends and cycles) in a dynamic setting. In this model, forecasters jointly update their beliefs about the two components: noisy information about one component is used to update beliefs about the other component. We present diagnostic empirical facts on forecasting behaviors and show that these facts are consistent with our model's predictions while contradicting those of existing models in the expectation formation literature. To validate our model, we exploit the Federal Reserve's 2012 adoption of explicit inflation targeting as a policy shock. Structural estimation reveals that this policy change altered the underlying data-generation process, and the corresponding changes in forecasting behavior indeed align with our model's predictions. Finally, we revisit the standard Forecast Error-Forecast Revision regression approach in this literature. We examine its robustness within our enriched framework and reveal that trend-cycle confusion can interact with behavioral bias and generate horizon-dependent overreaction patterns documented in empirical studies.

Keywords. expectation formation, forecasting, overconfidence, inflation expectation, Survey of Professional Forecasters.

JEL Classification. D83, D84,E37

*Heng CHEN: hengchen@hku.hk; Yicheng LIU: yicheng61@connect.hku.hk. The paper was previously circulated as "Trend, Cycle and Expectation Formation."

1 Introduction

In much of the existing literature on expectation formation, researchers assume that macroeconomic variables consist of one stationary component (e.g., Coibion and Gorodnichenko 2015; Bordalo et al. 2020). In the literature on signal extraction, researchers typically assume that the state variable comprises a random walk aggregate component and a transitory idiosyncratic component (e.g., Lucas and Prescott 1978; Collard et al. 2009; Lorenzoni 2009). However, few studies have investigated how forecasters simultaneously handle trends and cycles in their expectation formation process. We address this gap by characterizing how forecasters update beliefs, form expectations, and make forecasts when macroeconomic variables contain trend components that cannot be perfectly distinguished from cyclical components.

Our contributions are twofold. First, we provide empirical evidence showing how forecasting behaviors vary across different forecast horizons—evidence that contradicts assumptions commonly used in existing models. Second, we fully characterize a dynamic setting where two persistent components (trends and cycles) cannot be perfectly disentangled. Unlike previous work, our framework allows both components to be unobservable and persistent, creating a more realistic trend-cycle confusion mechanism that accounts for our documented empirical patterns.

We begin our empirical analysis using the Survey of Professional Forecasters (SPF), which collects individual-level forecasts for macroeconomic variables at both short and long horizons.[1] First, we examine the covariance between changes in long-run and short-run cyclical forecasts at the forecaster level. We focus on this empirical moment because it maps directly to theoretical predictions and helps distinguish between competing models.

Specifically, we consider three-year-ahead forecasts for macroeconomic variables, such as the real GDP growth rate and the unemployment rate, as long-run forecasts. The difference between the h-quarters ahead forecast of a relevant macroeconomic variable and its three-year-ahead forecast is defined as the cyclical forecast, capturing short-run deviations from the long-run forecast. We then construct 'across-period changes' in both long-run and cyclical forecasts for each forecaster. Changes in long-run forecasts are calculated as the difference between their three-year-ahead forecasts in quarters t and $t-1$. Similarly, we calculate changes in cyclical forecasts. By construction, changes in long-run forecasts reflect belief changes in both the trend and cyclical components, while changes in cyclical forecasts are proportional to belief changes in the cyclical component.

Models that assume either an observable trend or a transitory cyclical component

[1] The SPF offers key advantages over alternative datasets: Blue Chip forecasts are limited to six quarters ahead without long-run projections, while Consensus Economics only provides long-run forecasts at the consensus level.

predict a non-negative covariance between changes in long-run forecasts and cyclical forecasts. This occurs because in these models, forecasters update their beliefs regarding the two components independently. Furthermore, these models predict that this covariance should decrease as h increases, converging to zero when h approaches three years, since the cyclical component plays a diminishing role over longer horizons.

However, our empirical findings contradict these theoretical predictions. For both real GDP growth and the unemployment rate in the SPF data, the covariance of interest is negative and increases as h increases. In other words, not only is the sign of the covariance opposite to what existing models predict, but its pattern over the forecast horizon h is also reversed.

Second, we examine how the cross-sectional dispersion of forecasts varies over the forecast horizon. Models that assume either an observable trend or a transitory cyclical component predict that forecast dispersion among forecasters should monotonically decrease as the forecast horizon increases. This is because disagreement among forecasters, caused by heterogeneous information about cyclical components, would diminish as the forecast horizon extends.[2]

Using the SPF data, we observe that for most macroeconomic variables (after being transformed into growth rates), forecast dispersion increases as the forecast horizon extends from zero to four quarters ahead. Additionally, we examine year-level forecast dispersion for real GDP growth and the unemployment rate over a longer forecast horizon and show that it increases as the horizon expands from one to three years. Interestingly, for inflation expectations, one of the most important macroeconomic variables, forecast dispersion decreases over horizons. These findings present a challenge for existing models and raise the question of how to reconcile both patterns of increasing and decreasing forecast dispersion across different variables and time horizons within one coherent framework.

Motivated by these findings, we propose an otherwise standard forecasting model that explicitly incorporates a non-stationary, unobservable trend component in the data generation process. Specifically, in this model, the state variable consists of a non-stationary random walk trend component and a cyclical component that follows the standard AR(1) process. The goal of forecasters is to minimize the squared error of their forecasts. The actual value of the state, which is the sum of these two components, is publicly announced and observed by forecasters at the end of each period.

The key assumption is that forecasters cannot directly observe the actual realizations of the trend and cyclical components. Instead, in each period, they receive two private noisy signals on the trend and cyclical components, respectively. This means

[2]For example, if the forecasted variable is assumed to follow a stationary data generation process (e.g., an AR(1) process with a constant long-run mean), when the forecast horizon is long enough, all forecasts should converge to that long-run mean, and the forecast dispersion would approach zero.

that they are unable to differentiate the two components perfectly and must make inferences about them based on imperfect information.

In such a setting, forecasters need to update their beliefs about the trend and cyclical components *twice* in each period. At the beginning of each period, forecasters receive private signals regarding the trend and cyclical components and then revise their beliefs on each component. Forecasters use this set of posterior beliefs to make forecasts that minimize the expected forecasting errors. At the end of each period, the actual state value is disclosed, which is informative about both the trend and cyclical components. Consequently, forecasters must update their beliefs again, making revisions to their beliefs about the two components.

In this model, forecasters do not update their beliefs about the trend and cyclical components independently. In other words, they are rationally confused. Specifically, in the presence of this confusion mechanism, a strong signal about the cyclical component creates a positive surprise, which plays a dual role. First, it provides information about the cyclical component; therefore, forecasters revise their posterior beliefs regarding the cyclical component upwards from the prior beliefs inherited from the previous period. This is the standard belief updating mechanism. Second, such a positive surprise about the cyclical component is also useful for updating beliefs about the trend component. Forecasters rationally interpret the positive surprise as indicating they likely underestimated the cyclical component previously. Consequently, they would conclude that they had likely overestimated the trend component and would revise their current beliefs regarding the trend component downward.

In summary, the confusion between trend and cyclical components leads forecasters to rationally update their beliefs about these components in opposite directions. This mechanism gives rise to a negative covariance between the two beliefs. In the data, the constructed covariance between changes in long-term forecasts and changes in cyclical forecasts is proportional to the sum of the negative covariance of beliefs and the variance of beliefs about the cyclical component. When the confusion mechanism dominates, the covariance between changes in long-term and cyclical forecasts can be negative. Furthermore, as the forecast horizon h used to construct the cyclical forecasts increases, the constructed change in cyclical forecasts reflects a smaller proportion of the changes in cyclical components. Therefore, the covariance of changes in forecasts should also diminish in magnitude as h increases.

This mechanism can also account for the observed increase in forecast dispersion over horizons. In this model, for any forecast horizon, the dispersion of forecasts can be broken down into three parts: the dispersion caused by heterogeneous beliefs about the cyclical component, the dispersion caused by heterogeneous beliefs about the trend component, and the covariance between these beliefs. The first part, the dispersion caused by heterogeneous beliefs about the cyclical component, always de-

creases over the forecast horizon, as the cyclical component becomes less influential for longer-term forecasts. The second part, the dispersion caused by heterogeneous beliefs about the trend component, remains constant over the forecast horizon, as the trend component is equally important for all horizons.

The third part, characterized by the *negative covariance* of cross-forecaster mean beliefs regarding the two components, is a novel aspect of the model. It stems from forecasters' use of signals regarding one component to update their beliefs about the other component. Furthermore, its importance diminishes over the forecast horizon as the cyclical component itself becomes less influential in forecasting. Therefore, the overall forecast dispersion could either increase or decrease over horizons. We show that forecast dispersion increases under the condition that the trend is neither too volatile nor too stable.

A few comments on our model are in order. First, while we choose to model this rational confusion mechanism in a trend-cycle framework to address specific empirical patterns and validate our approach with data, the underlying mechanism is more general. Indeed, this confusion mechanism extends to situations where both components exhibit persistence without requiring a random walk component. Second, it is important to note that the data generating process we specify represents the perceived process by forecasters rather than necessarily capturing the objective process, which remains unobservable to them.

Model Validation: Explicit Inflation Targeting. Our theoretical framework generates distinct forecasting patterns that vary with the underlying parameter space. To validate these predictions, we leverage a natural experiment–the implementation of explicit inflation targeting in 2012–which altered the data-generating process for inflation. This policy shift provides an ideal testing ground for our model. Our analysis demonstrates that the observed changes in forecasting behaviors following this policy implementation align with our theoretical predictions, lending strong support to our proposed mechanism of rational confusion.

Model Application: FE-FR Regression. We revisit two seminal studies in the expectation formation literature within our framework. First, we re-examine the consensus-level Forecast Error-Forecast Revision (FE-FR) regression proposed by Coibion and Gorodnichenko (2015) to quantify information friction. Our analysis reveals that this coefficient captures not only the information friction due to imperfect information but also the new friction of trend-cycle confusion and the effects of observable past data. Importantly, we establish that this coefficient provides a lower bound on the total information frictions present in the data.

Second, we extend our model to the individual-level FE-FR regression introduced by Bordalo et al. (2020) by incorporating forecaster overconfidence. This extension generates novel predictions: overconfidence in trend signals can generate a larger

overreaction in long-run forecasts – a pattern consistent with an empirical anomaly documented in the literature.

Literature Review. This paper contributes to the literature on expectation formation in particular and information friction in general. First, a key innovation of our work is the incorporation of non-stationary trend components into the data generation process, which cannot be separated perfectly from cyclical components. This is the point of departure from the standard approach in the expectation formation literature (Coibion and Gorodnichenko 2015; Bordalo et al. 2020; Angeletos and Huo (2021); Broer and Kohlhas 2024; Huo et al. 2024) which assumes stationary data-generating processes.[3] This extension is both realistic and empirically relevant, as substantial evidence documents the presence of non-stationary trends in critical macroeconomic variables, including GDP growth (Stock and Watson 1998) and unemployment rates (Blanchard and Summers 1986).

Second, our model contributes to the existing literature on signal extraction problems in macroeconomics. Existing works focus on cases where forecasters cannot distinguish between persistent and transitory components (Muth 1960; Lucas 1972; Lucas and Prescott 1978; Collard et al. 2009; Lorenzoni 2009; Bostanci and Ordoñez 2024;Xie 2023). Our model differs in that, in a noisy information framework, forecasters need to separate two persistent components in a dynamic setting, which generates negatively correlated belief updates between the components.

Third, our evidence-motivated theoretical model, while utilizing a trend-cycle framework, differs from related quantitative works in this area. Unlike Farmer et al. (2024), who focus on model uncertainty within a Bayesian learning approach and address consensus forecast anomalies, our work employs a noisy information paradigm to examine heterogeneity in individual forecasting behaviors across different horizons, including cross-forecaster dispersion patterns. Similarly, while Fisher et al. (2025) develop a behavioral model to explain long-run inflation expectation anomalies, our work presents a fully rational confusion mechanism that addresses a broader set of empirical regularities applicable to macroeconomic variables generally.

Finally, our work addresses the documented phenomenon that forecast dispersion tends to be larger in the long run. In the previous literature, studies have explained this pattern through either behavioral biases (Lahiri and Sheng 2008 and Patton and Timmermann 2010) or sticky information frameworks (Andrade et al. 2016). Our model offers a novel alternative, as the confusion mechanism we propose is fully rational rather than behavioral.

[3]New contributions to this literature further expand its scope. For instance, Kohlhas and Walther (2021) explore why individual forecast errors are negatively correlated with current realizations, while Rozsypal and Schlafmann (2023) examine how forecaster characteristics influence individual forecast errors. Chen et al. (2024) study individuals' heterogeneous overreaction to shocks of various properties.

2 Evidence

This section presents two key empirical findings from the U.S. Survey of Professional Forecasters (SPF). First, we document a negative covariance between changes in forecasters' long-term and cyclical forecasts. Second, we show that forecast dispersion among forecasters tends to increase with the forecast horizon for most macroeconomic variables.

2.1 Survey of Professional Forecasters Data

The Survey of Professional Forecasters (SPF) of the U.S. is a source of predictions made by professional forecasters regarding a broad range of macroeconomic variables. The data is collected quarterly and goes back to 1968Q4. The Fed of Philadelphia surveys approximately 35 professional forecasters each quarter, assigning a unique ID number to each forecaster to track their forecast history.

For each variable, a forecaster provides six predictions, including one back-cast toward the previous period, a now-cast (forecast for the current quarter), and forecasts for the subsequent four quarters. In addition, they are asked to provide The annual projection of this variable for the current year, and the next year. Since 1991Q4, the survey has included an extra question regarding the Consumer Price Index (CPI) for a ten-year forecast. Since 1992Q1, the first quarter survey has included an additional question about the GDP for a ten-year forecast, while since 1996Q3, the third quarter survey has incorporated an additional question regarding the natural unemployment rate. Starting from 2009, SPF has expanded to encompass year-level forecasts of the unemployment rate and real GDP for two- and three-year periods. Table 3 in Appendix provides a summary of the starting dates and frequency for each data series.

The survey is conducted before the end of each quarter, following the Bureau of Economic Analysis' (BEA) advance report of the national income and product accounts (NIPA) release. The BEA reports macroeconomic variables (e.g., GDP estimates) for the preceding quarter. At the beginning of the questionnaire, forecasters will be provided with the BEA reported value of the macro variable for the previous quarter. Therefore, when giving their predictions for current and future quarters, forecasters have access to information about the values of forecasted variables up to the last quarter.

In Appendix A.4, we use the European Central Bank's Survey of Professional Forecasts (ECB-SPF) as a robustness check. The ECB-SPF provides individual forecasts for unemployment, real GDP growth, and inflation at multiple horizons: current year, next year, two years ahead, and long-run. This comprehensive horizon coverage enables us to proxy individual cyclical beliefs quarterly. Both the US-SPF and ECB-SPF have advantages over alternative datasets: Blue Chip forecasts are limited to six quar-

ters ahead and lack long-run projections (except for inflation)[4], and Consensus Economics only reports long-run forecasts at the aggregate level.

2.2 Covariance: Changes in Long Term Forecasts and Cyclical Forecasts

Building on this dataset, the following section presents a novel empirical test that examines the covariance between changes in forecasters' long-term and cyclical forecasts across time. We will show that the covariance of these changes is informative about the process of expectation formation.

We start our investigation by constructing forecasters' long-run forecasts and cyclical forecasts. As discussed earlier, since 2009, the Survey of Professional Forecasters (SPF) has asked forecasters each quarter to report their long term forecasts for the unemployment rate and real GDP, precisely three years ahead. We employ forecaster i's three-year ahead forecast at quarter t, denoted as $F_{i,t}y_{t+3Y}$, to represent her long-run forecasts.[5] Furthermore, we utilize the deviation of forecaster i's forecast h period ahead at quarter t, denoted as $F_{i,t}y_{t+h}$, from the three-year ahead forecast as her cyclical forecasts. Specifically, forecaster i's cyclical forecasts is constructed as follows:

$$Cyc^h_{i,t} = F_{i,t}y_{t+h} - F_{i,t}y_{t+3Y}.$$

Then, we examine the covariance between the changes in the long-run forecasts and the cyclical forecasts:

$$COV^h_F = cov(F_{i,t}y_{t+3Y} - F_{i,t-1}y_{t-1+3Y}, Cyc^h_{i,t} - Cyc^h_{i,t-1}). \tag{1}$$

The first term on the right-hand side of Equation (1) represents the difference between three-year ahead forecasts for periods t and $t-1$. The second term corresponds to the change in cyclical forecasts between these two periods. The horizon $h = 0, 1, 2, 3, 4$ represents the forecast horizon for the short-term forecast, which is utilized to construct the forecasts on cyclical components.

If the trend is perfectly observable to forecasters, this covariance shall be positive. This is because changes in cyclical forecasts reflect changes in the cyclical components from quarter t to quarter $t-1$. Similarly, changes in long-term forecasts represent shifts in both the trend and cyclical components between these quarters. The covari-

[4]While Blue Chip derives inflation expectations from various indicators ranging from 3-month T-bills to 30-year T-bonds, the spread between these rates cannot be interpreted as cyclical beliefs.

[5]A possible concern is that three-year-ahead forecasts may not adequately represent long-run forecasts. To address this, we utilize two forecast series with longer horizons: ten-year forecasts for real GDP (available every first quarter since 1992Q1) and forecasts of the natural unemployment rate (available every third quarter since 1996Q3). In Appendix A.2, we demonstrate that three-year-ahead forecasts are highly correlated with those for longer horizons, making them reasonable representations of long-run forecasts. We do not use the ten-year forecasts for GDP and the natural unemployment rate in our analysis due to the coarse frequency of observations at the yearly level. Instead, we focus on three-year-ahead forecasts, which are available at the quarterly level.

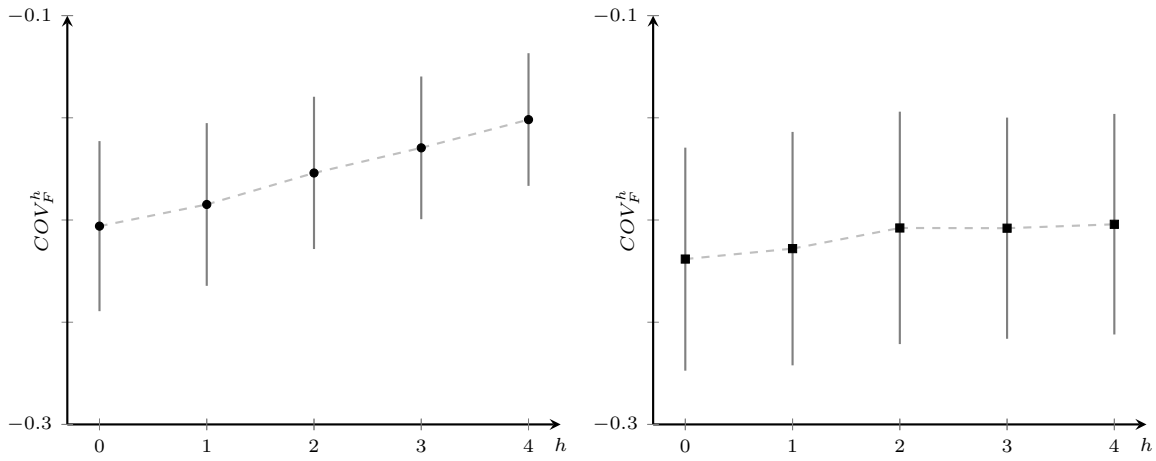

(a) Unemployment (b) Real GDP growth

Figure 1. *Covariance between the changes in long-run forecasts and cyclical forecasts across forecast horizon h. Note: This figure illustrates the covariance COV_F^h for the unemployment rate and real GDP growth across various forecast horizons h. The left panel shows the COV_F^h for the unemployment rate, while the right panel depicts the COV_F^h for real GDP growth. In both cases, the covariance is negative and statistically significant, increasing as the forecast horizon extends. The black dots represent the estimates, and the gray solid lines denote the 95% confidence intervals.*

ance must be positive, provided that the innovations in trend and cyclical components are uncorrelated. Furthermore, the covariance should decrease as h (i.e., the forecast horizon for the short-term forecast used to construct cyclical forecast) increases, since the changes in cyclical forecasts would be less proportional to changes in cyclical innovations when h is longer.

If the cyclical component is not persistent (i.e., $\rho = 0$), this covariance should be zero. This is because changes in long-term forecasts would only represent shifts in the trend between these quarters. This set of predictions is characterized in Section 4.4.

Figure 1 illustrates the covariance between changes in long-run forecasts and cyclical forecasts for both the unemployment rate and real GDP growth. The x-axis represents the forecast horizons set at $h = 0, 1, 2, 3, 4$. Figure 1(a) shows the COV_F^h for the unemployment rate, while Figure 1(b) depicts the COV_F^h for real GDP growth. We observe a negative and significant COV_F^h for both variables, with the covariance increasing as the horizon h expands. Details of this estimation are shown in Table 4.

These findings suggest that when a forecaster updates her long-run forecast upward, she tends to simultaneously revise her cyclical forecast downward. The empirical results reveal a pattern contrary to the predictions of the observable-trend model: not only is the covariance negative instead of positive, but it also increases over the horizon h rather than decreases.

In Appendix A.4, we present estimation results using ECB-SPF data for the unemployment rate, real GDP growth, and inflation. These results are consistent with the

Table 1. *Forecast dispersion over forecast horizon*

	Dependent Variable: Forecast Dispersion				
	Variance of forecasts		50 percentile difference		
	β_1	SE	β_1	SE	Obs
Forecast Variable	(1)	(2)	(3)	(4)	
Nominal GDP	0.337***	0.026	0.204***	0.008	1,025
Real GDP	0.242***	0.022	0.162***	0.007	1,025
GDP price index inflation	0.118***	0.008	0.119***	0.004	1,025
Real consumption	0.125***	0.013	0.127***	0.006	770
Industrial production	0.860***	0.062	0.320***	0.014	1,025
Real nonresidential investment	1.647***	0.127	0.497***	0.018	770
Real residential investment	6.021***	0.547	0.932***	0.039	770
Real federal government consumption	1.284***	0.102	0.393***	0.019	770
Real state and local government consumption	0.317***	0.028	0.210***	0.009	770
Housing start	0.004***	0.000	0.020***	0.001	1,024
Unemployment	0.034***	0.002	0.081***	0.003	1,014
Inflation (CPI)	-0.066***	0.021	-0.073***	0.012	770
Three-month Treasury rate	0.091***	0.010	0.132***	0.007	770
Ten-year Treasury rate	0.045***	0.001	0.094***	0.003	560

Note: This table shows results from estimating Equation (2). The sample period is from 1968Q4 to 2019Q4. In column (1), the dependent variable is the variance of forecasts across forecasters. In column (3), we use the difference between the 25% percentile and 50% percentile. Standard errors are clustered at the year-quarter level.

pattern in Figure 1, where all three variables exhibit negative covariance that increases with the forecast horizon h.

2.3 Forecast Dispersion over Forecast Horizon

In this section, we explore whether the dispersion in forecasts among forecasters varies as the forecast horizon extends. This analysis provides insights into the role of beliefs concerning trends and cycles. If the trend is observable or the cyclical component lacks persistence, forecast dispersion should decrease monotonically as the forecast horizon increases, regardless of whether we examine short-term forecasts (within a year) or longer-term forecasts. This set of predictions will be characterized in Section 4.4.

First, we investigate the short-term forecasts, for which we have forecast data for most macroeconomic variables. Using SPF data, we estimate the following equation:

$$\text{Forecast dispersion}_{th} = \alpha + \beta_1 h + \epsilon_{th}, \tag{2}$$

where $\text{Forecast dispersion}_{th}$ represents the cross-forecaster dispersion in forecasts $F_{i,t}y_{t+h}$ provided by forecaster i at period t for h quarters ahead and the forecast horizon is defined as $h = 0, 1, 2, 3, 4$. The standard error is clustered at the year-quarter level.

We consider two measures of forecast dispersion: the variance of forecasts across forecasters and the difference between the 75th percentile and the 25th percentile. We estimate Equation (2) using all available macroeconomic variables. The estimated coefficient β_1 is of particular interest and is presented in Table 1.

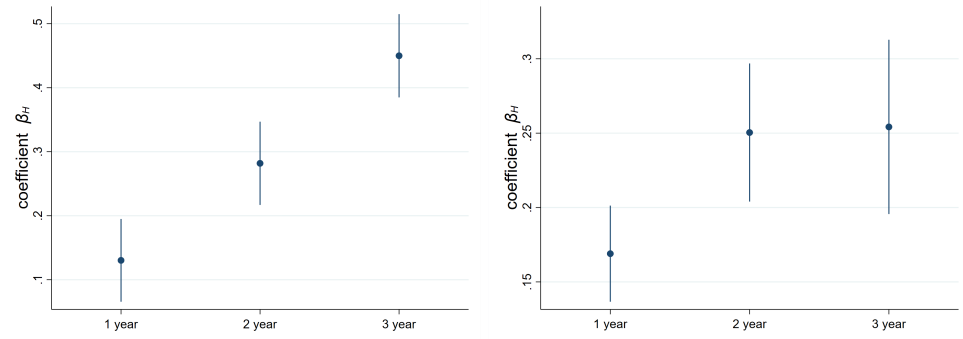

(a) Unemployment rate (b) Real GDP growth

Figure 2. *Dispersion of the year-level forecasts. Note: The figure presents the estimation results from Equation (3). The panel on the left displays the estimated coefficients for the unemployment rate, while the panel on the right shows those for real GDP growth. The sample period spans from 2009Q1 to 2019Q4. In both cases, β_H is greater than zero and increases as H increases, indicating larger dispersion as the forecast horizon expands.*

Column (1) of Table 1 presents the results using forecast variance as the measure of forecast dispersion. The coefficient for the forecast horizon h is positive ($\beta_1 > 0$) and statistically significant for most variables, indicating that forecasts among forecasters become more dispersed as the forecast horizon increases. The only exception is inflation. We will revisit the analysis of inflation expectations in section 5. In column (3), we repeat our estimations using the difference between the 75th and 25th percentiles as the measure of forecast dispersion. The results are rather similar. To confirm that the pattern is robust to the inclusion of time fixed effect, we report the estimation results with year-quarter fixed effect in Table 6. In addition, using the coefficient of variation as the measure of forecast dispersion, the results would be very similar.

Second, we investigate the longer-term forecasts, for which we have forecast data for fewer variables. Specifically, we focus on a subset of variables with annual forecast data that spans an extended horizon. Starting from 2009Q1, the U.S. Survey of Professional Forecasters (SPF) includes forecasts for real GDP and the unemployment rate one year, two years, and three years into the future. We utilize this dataset to estimate the following specification:

$$\text{Forecast dispersion}_{tH} = \alpha_2 + \sum_{H=1}^{3} \beta_H \, \text{horizon}_H + \epsilon_t, \tag{3}$$

where $\text{Forecast dispersion}_{tH}$ is the dispersion of forecasts of horizon H across all forecasters and horizon_H is a dummy variable for horizon H, taking the value 1 if the forecast horizon is $H = 1$ year, 2 years, or 3 years ahead; and 0 otherwise. The coefficient β_H captures the difference in forecast dispersion between forecasts H years

ahead and current year predictions ($H = 0$).

Figure 2 presents the estimation results. Figure 2(b) shows results for real GDP, while Figure 2(a) displays results for the unemployment rate. In both cases, the coefficients β_H are positive and increase with the forecast horizon. These findings also contradict the predictions of the observable-trend model, which states that dispersion should decrease monotonically.

In the literature, several studies have investigated this particular pattern, which offer similar findings that are inconsistent with the observable-trend model. Lahiri and Sheng (2008) use the *Consensus Forecasts* data and show that the forecast dispersion of real GDP growth is larger in a longer forecast horizon for all the G7 countries. Patton and Timmermann (2010) utilize the same data and find that both the forecast dispersion regarding the U.S. GDP growth and inflation is higher at longer horizons. Andrade et al. (2016) study the data from Blue Chip Survey and find a steady increase in the dispersion of Federal Fund rate forecasts as the forecast horizon extends.

3 Forecasting Model with Trend-cycle Confusion

3.1 Setup

Utility function. In this model, there exists a continuum of forecasters, indexed by $i \in [0, 1]$, who make forecasts about a stochastic state variable y_t. The objective of the forecasters is to minimize forecasting errors. We consider a standard quadratic utility function, which is given by:

$$U(F_{i,t}y_{t+h}) = -(F_{i,t}y_{t+h} - y_{t+h})^2, \tag{4}$$

where y_{t+h} is the actual value of the state in period $t + h$ and $F_{i,t}y_{t+h}$ denotes the forecast made by forecaster i at period t for the state h periods in the future.

Data generation process. We assume that the state variable y_t is composed of two components: a trend component, μ_t, representing long-term trend, and a cyclical component, x_t, capturing short-term fluctuations. In particular, the trend follows a random walk process, while the cycle is modeled as an AR(1) process. Specifically, the data generation process for the state can be described as follows:

$$\begin{aligned} y_t &= \mu_t + x_t, \\ \mu_t &= \mu_{t-1} + \gamma_t^{\mu}, \\ x_t &= \rho x_{t-1} + \gamma_t^{x}, \end{aligned} \tag{5}$$

where ρ is the persistence for the AR(1) process and γ_t^{μ} and γ_t^{x} are the innovations of the trend and cyclical components, both of which are normally distributed with zero mean and variances of σ_{μ}^2 and σ_x^2, respectively, i.e.,$\gamma_t^{\mu} \sim N(0, \sigma_{\mu}^2)$ and $\gamma_t^{x} \sim N(0, \sigma_x^2)$.

We use $\boldsymbol{\theta_t} = (\mu_t, x_t)'$ to denote the state components in period t. Consistent with the previous literature, we assume that the data generating process (DGP) is common knowledge for all forecasters.[6]

In each period, forecasters receive private noisy signals for each component, that is, $\boldsymbol{s_{i,t}} = (s^{\mu}_{i,t}, s^{x}_{i,t})'$, where[7]

$$s^{\mu}_{i,t} = \mu_t + \epsilon_{i,t}; \quad \text{and} \quad s^{x}_{i,t} = x_t + e_{i,t}. \tag{6}$$

We assume that the error terms of the signals are independent and normally distributed. The variance-covariance matrix of i's private signals is given by:

$$\boldsymbol{\Sigma_s} = \begin{pmatrix} \sigma^2_{\epsilon} & 0 \\ 0 & \sigma^2_{e} \end{pmatrix}.$$

At the end of each period t, we allow forecasters to observe the actual state variable y_t but not the trend and cyclical components. Therefore, upon the announcement of the actual state value, forecasters revise their beliefs regarding the trend and cyclical components. The updated beliefs about the two components become the prior beliefs for the next period.

Throughout the paper, we use $\boldsymbol{\theta}^i_{1,t}$ to represent forecaster i's posterior belief after forecaster i receive signals about the trend and cyclical components in period t (i.e., the first update). We use $\boldsymbol{\theta}^i_{2,t}$ to represent forecaster i's posterior belief after they observe the actual realization of the state in period t (i.e., the second update). The subscript 1 and 2 stand for the first and second updating in period t, respectively. We summarize the timeline of our setting in Figure 3:

- At the beginning of period t, forecaster i is endowed with the prior belief $\boldsymbol{\theta}^i_{2,t-1}$, which is the posterior of the second updating from the period $t-1$.
- Forecaster i observes the private signal $\boldsymbol{s_{i,t}}$ and then update her belief accordingly (the first updating).
- Given the updated beliefs $\boldsymbol{\theta}^i_{1,t}$, forecasters choose their optimal forecasts of the current and future period $F_{i,t}y_{t+h}$.

[6] In Appendix B.3, we discuss the scenario in which a common shock affects both the trend and cyclical components. This specification resembles that in Delle Monache et al. (2024). We demonstrate that this setting cannot produce the observed empirical patterns if the trend component is observable.

[7] Trend signals, reflecting long-run economic shifts, include announcements of structural reforms (e.g., deregulation), demographic projections, technological breakthroughs (e.g., AI advancements), changes to central bank inflation targets, and long-term policy framework adjustments. Conversely, cycle signals, indicating short-term fluctuations, include temporary supply chain disruptions, extreme weather events, fiscal stimulus measures (e.g., tax rebates), and inventory cycle updates. Forecasters also leverage proprietary research, such as business surveys and alternative data analysis, to be informed about both trend and cycle components.

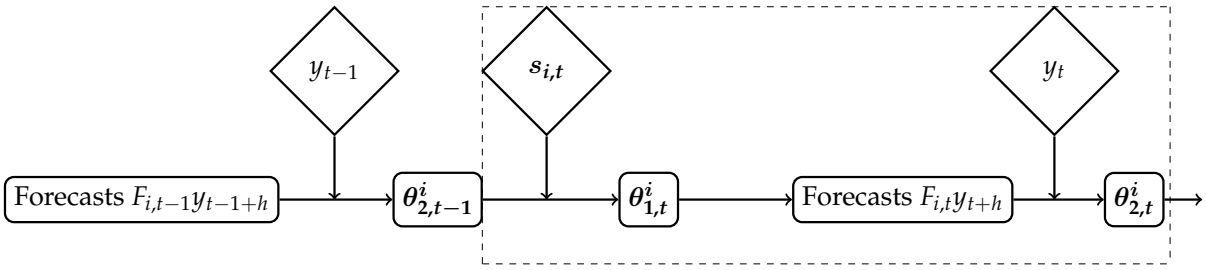

Figure 3. *Timeline. In each period t, forecaster i will update her beliefs twice. First, based on the observed private signals, forecaster i adjusts her beliefs and provides forecasts for the current and future periods, i.e., $F_{i,t}y_{t+h}$. Second, forecaster i revises her beliefs regarding the trend and cycle upon observing the actual realization of the state variable. The diamond boxes represent exogenous information flow. The squared boxes stands for the forecaster i's beliefs.*

- At the end of period t, y_t is revealed.
- Forecasters revise their beliefs again, forming beliefs $\boldsymbol{\theta}^i_{2,t}$ (the second updating).

Several important clarifications about our model are worth highlighting. First, the data generating process specified in Equation (5) should be interpreted as the perceived process by forecasters, rather than necessarily representing the objective one, which remains unobservable to them. Second, while we model the trend component as a non-stationary random walk both for simplicity and to better fit macroeconomic data, this specific assumption is not critical to our main results. The key feature is the presence of multiple persistent components that are not perfectly distinguishable from one another, creating a signal extraction challenge for forecasters. In Section 4.4, we generalize our framework to allow both components to be persistent, and we provide complete characterizations and proofs for this more flexible specification in Appendix B.2. Finally, we focus on a univariate setting where forecasters update their predictions for each macroeconomic variable individually. This modeling choice is supported by empirical evidence in Wang and Hou (2024), which supports the realism of this forecasting behavior.

3.2 Characterization

In this section, we turn to the characterization of forecasters' optimal forecasts. We start our analysis by considering the posterior belief obtained from the second update in period $t-1$, which is the prior belief of forecaster i at the beginning of period t:

$$\boldsymbol{\theta}^i_{\mathbf{2,t-1}} = (\mu^i_{2,t-1}, \rho x^i_{2,t-1})',$$

where $\mu^i_{2,t-1}$ and $x^i_{2,t-1}$ are forecaster i's beliefs about trend and cyclical components at the end of period $t-1$, respectively. Let $z_{i,t-1}$ be forecaster i's error in her belief regarding the trend in period $t-1$.

Lemma 1. Suppose the error term $z_{i,t-1}$ in period $t-1$ is normally distributed, then $z_{i,t}$ must also be normally distributed. The set of beliefs $\mu^i_{2,t-1}$ and $x^i_{2,t-1}$ can always be written in the form:

$$\mu^i_{2,t-1} \equiv \mu_{t-1} + z_{i,t-1} \quad and \quad x^i_{2,t-1} \equiv x_{t-1} - z_{i,t-1}, \tag{7}$$

which implies:

$$\mu^i_{2,t-1} + x^i_{2,t-1} = y_{t-1}.$$

The proof and subsequent proofs are collected in Appendix B. In the following, we call $z_{i,t-1}$ the *separation error*. First, if the separation error follows a normal distribution in one particular period, it will continue to be normally distributed indefinitely, given that both the state innovations and signals are also normally distributed. Second, given the actual y_{t-1} is observed at the end of $t-1$, the normality assumption and the Bayes' rule requires that beliefs regarding the two components $\mu^i_{2,t-1}$ and $x^i_{2,t-1}$ must sum up to y_{t-1}. That is, the error terms in the two beliefs are of the same magnitude but opposite in sign.

Denote the variance of $z_{i,t-1}$ as $\sigma^2_{z,t-1}$, then the variance-covariance matrix of $\boldsymbol{\theta^i_{2,t-1}}$ follows:

$$\boldsymbol{\Sigma}_{\boldsymbol{\theta^i_{2,t-1}}} = \begin{pmatrix} \sigma^2_{z,t-1} + \sigma^2_\mu & -\rho\sigma^2_{z,t-1} \\ -\rho\sigma^2_{z,t-1} & \rho^2\sigma^2_{z,t-1} + \sigma^2_x \end{pmatrix}.$$

The sub-diagonal term $-\rho\sigma^2_{z,t-1}$ in the covariance matrix is negative. Intuitively, if a forecaster believes that the trend is stronger than it actually is (i.e., forecasting error on the trend component is positive), she will tend to believe that the cyclical component is weaker than it actually is, and vice versa. Note that when forecasters can perfectly distinguish between the trend and cyclical components, the corresponding sub-diagonal term will be zero. We will refer to $\sigma^2_{z,t}$ as the extent of confusion in distinguishing between the trend and cyclical components.

Lemma 2. There exists a unique steady state σ^2_z for the variance $\sigma^2_{z,t}$.

The variance $\sigma^2_{z,t}$ always converges to a steady-state value, σ^2_z. To understand why the variance of the error term, or the extent of confusion, converges, we observe two opposing forces resulting from the observation of actual data y_t. On the one hand, the change in state provides information about the cyclical component in the last period, given by $y_t - y_{t-1} = -(1-\rho)x_{t-1} + \gamma^x_t + \gamma^\mu_t$. This assists forecasters in separating the cyclical component from the trend, reducing their confusion. On the other hand, because y_t comprises both components, forecasters use the observation of the state and their beliefs about trends (i.e., $y_t - \mu^i_{1,t}$) to revise their beliefs regarding the cyclical component x_t, thereby increasing their confusion.

When $\sigma^2_{z,t-1}$ is large, it implies lower-quality prior beliefs and therefore a lower quality of $\mu^i_{1,t}$. Consequently, the second force becomes less important, and the first force dominates, leading to a smaller $\sigma^2_{z,t}$. Conversely, when $\sigma^2_{z,t-1}$ is small, the second force dominates, resulting in an increase in the extent of confusion. Therefore, the steady-state value of σ^2_z always exists.

Throughout the paper, we assume that the separation error z_i has converged to the steady state, given the results are qualitatively similar when the error term has not converged.

Assumption 1. The variance of separation error has converged to the steady state σ^2_z.

In the following, we present how forecasters update their beliefs and make forecasts by following the timeline of events. The first step involves characterizing the process of belief updating after forecasters receive their private signals regarding trends and cycles. In period t, after acquiring the private signals $\boldsymbol{s}_{i,t}$, forecaster i updates her beliefs on the trend and cyclical components and form her beliefs $\boldsymbol{\theta}^i_{1,t}$, which is joint-normally distributed. The expectations of these beliefs are given by:

$$\boldsymbol{\theta}^i_{1,t} = \boldsymbol{\theta}^i_{2,t-1} + \boldsymbol{\kappa} \times (\boldsymbol{s}_{i,t} - \boldsymbol{\theta}^i_{2,t-1}), \tag{8}$$

where $\boldsymbol{\kappa}$ is the Kalman gain and $(\boldsymbol{s}_{i,t} - \boldsymbol{\theta}^i_{2,t-1})$ is the surprise from signals:

$$\boldsymbol{\kappa} = \begin{pmatrix} \frac{V+\sigma^2_e(\sigma^2_z+\sigma^2_\mu)}{\Omega} & -\frac{\rho\sigma^2_\epsilon\sigma^2_z}{\Omega} \\ -\frac{\rho\sigma^2_e\sigma^2_z}{\Omega} & \frac{V+\sigma^2_\epsilon(\sigma^2_x+\rho^2\sigma^2_z)}{\Omega} \end{pmatrix} \quad \text{and} \quad \boldsymbol{s}_{i,t} - \boldsymbol{\theta}^i_{2,t-1} = \begin{pmatrix} s^\mu_{i,t} - \mu^i_{2,t-1} \\ s^x_{i,t} - \rho x^i_{2,t-1} \end{pmatrix}.$$

The variance-covariance matrix of $\boldsymbol{\theta}^i_{1,t}$ is given by:

$$(\boldsymbol{\Sigma}_{\boldsymbol{s}}^{-1} + \boldsymbol{\Sigma}^{-1}_{\boldsymbol{\theta}^i_{2,t-1}})^{-1} = \begin{pmatrix} \text{Var}^T & \widetilde{COV} \\ \widetilde{COV} & \text{Var}^C \end{pmatrix} = \begin{pmatrix} \frac{\sigma^2_\epsilon[\Omega-\sigma^2_\epsilon(\sigma^2_x+\sigma^2_e+\rho^2\sigma^2_z)]}{\Omega} & -\frac{\rho\sigma^2_e\sigma^2_\epsilon\sigma^2_z}{\Omega} \\ -\frac{\rho\sigma^2_e\sigma^2_\epsilon\sigma^2_z}{\Omega} & \frac{\sigma^2_e[\Omega-\sigma^2_e(\sigma^2_\epsilon+\sigma^2_\mu+\sigma^2_z)]}{\Omega} \end{pmatrix}, \tag{9}$$

where Ω and V are positive constants:

$$\Omega = (\sigma^2_z + \sigma^2_\mu + \sigma^2_\epsilon)(\sigma^2_x + \sigma^2_e + \rho^2\sigma^2_z) - \rho^2\sigma^4_z \quad \text{and} \quad V = (\sigma^2_z + \sigma^2_\mu)(\sigma^2_x + \rho^2\sigma^2_z) - \rho^2\sigma^4_z.$$

The Kalman gain matrix $\boldsymbol{\kappa}$ has two parts. The elements on the main diagonal resemble those in the standard belief updating. That is, forecasters use signals about the trend (cycle) to update their beliefs on the trend (cycle).

When there is no confusion (i.e., σ^2_z goes to zero), the model reduces to the standard Bayesian case. In this scenario, the Kalman gain for the trend component reduces

to $\sigma_\mu^2/(\sigma_\mu^2+\sigma_\epsilon^2)$, and for the cyclical component, it reduces to $\sigma_x^2/(\sigma_x^2+\sigma_e^2)$. When there is confusion (i.e., $\sigma_z^2 > 0$), the Kalman gain becomes larger than the Bayesian case without confusion. In other words, the confusion mechanism leads to less precise prior beliefs, and forecasters rely more on the signals, which provide new information. A similar argument holds true for the Kalman gain for the cyclical component.

Crucially, the non-zero elements on the sub-diagonal of the Kalman gain matrix, i.e., $\boldsymbol{\kappa}_{1,2}$ and $\boldsymbol{\kappa}_{2,1}$, distinguish our model from the observable-trends model, where the counterpart terms are zero. This indicates that in our framework, forecasters incorporate information about the trend (cycle) component when updating their beliefs about the cyclical (trend) component. Consider a scenario where the private signal indicates that the cyclical component is stronger than the forecaster's prior belief. This situation could arise from three possibilities: Firstly, it might reflect a substantial positive innovation in the cyclical component itself. Secondly, it could be due to positive noise in the signal. Thirdly, it might suggest that the actual value of the cyclical component in the previous period was larger than what the forecaster believed. As forecasters cannot know the true value of each component with certainty, they will adjust their prior beliefs by increasing their estimate of the cyclical component from the last period and correspondingly decreasing their estimates of the trend component for both the last and current periods.

The variance-covariance matrix in Equation (9) warrants further discussion. Firstly, the elements on the main diagonal correspond to the perceived variance of the trend and cyclical components, which are influenced by the confusion mechanism. These variances are larger compared to the case where there is no confusion (i.e., the components can be perfectly observed). We denote them as Var^T and Var^C, respectively.

Secondly, the elements on the sub-diagonal components are non-zero and negative. That is, forecasters cannot perfectly distinguish between the trend and cycle, which gives rise to a negative covariance between the beliefs of these two components. Intuitively, when there are strong positive signals about the cyclical component, forecasters will simultaneously revise the cyclical component upward and the trend component downward. We denote this covariance of beliefs as $\widetilde{\text{COV}}$.

The second step is the stage of making forecasts. Forecaster i makes a series of forecasts about the state in h periods ahead. Under a quadratic utility function, her optimal prediction is the expected value of the state variable.

Lemma 3. The optimal forecast of forecaster i over horizon h is determined by their beliefs of trend and cyclical components, i.e.,

$$F_{i,t}y_{t+h} = E_{i,t}[\mu_t + \rho^h x_t] = \mu_{1,t}^i + \rho^h x_{1,t}^i.$$

This lemma says that the trend and cyclical beliefs play different roles over forecast

horizons: the trend belief consistently influences predictions across all horizons, while the influence of the cyclical belief diminishes as the forecast horizon extends.

The final step involves forecasters revising their beliefs again upon observing the actual value of the current state (y_t). This set of posterior beliefs becomes the prior beliefs for the next period. The forecasting error present in this set of posterior beliefs is the separation error ($z_{i,t}$). Lemma 4 characterizes its construction.

Lemma 4. Upon observing the actual state value y_t, the separation error $z_{i,t}$ present in the posterior beliefs is given by:

$$z_{i,t} = \frac{(\text{Var}^T + \widetilde{\text{COV}})(x_t - x^i_{1,t}) - (\text{Var}^C + \widetilde{\text{COV}})(\mu_t - \mu^i_{1,t})}{(\text{Var}^T + \widetilde{\text{COV}}) + (\text{Var}^C + \widetilde{\text{COV}})}. \tag{10}$$

The extent of confusion σ_z^2 increases as σ_μ^2, σ_x^2, σ_e^2, and σ_ϵ^2 increase, converges to zero if any of these parameters goes to zero and is also bounded:

$$0 \leq \sigma_z^2 \leq \min\{\text{Var}^C, \text{Var}^T\}. \tag{11}$$

Recall that Var^T and Var^C represent the variances of forecasters' posterior beliefs regarding the trend and cyclical components, respectively, while $\widetilde{\text{COV}}$ denotes the corresponding covariance between the two components, as shown in Equation (9).

Lemma 4 states that the separation error after forecasters observe the actual state, is a weighted combination of the error terms in forecasters' beliefs regarding the trend and cyclical components *before* they observe the actual state. If they over-predict the trend component (i.e., $\mu_t - \mu^i_{1,t} < 0$), then $z_{i,t}$ tends to be positive. Conversely, if they over-predict the cyclical component (i.e., $x_t - x^i_{1,t} < 0$), then $z_{i,t}$ tends to be negative.[8]

Note that after observing the actual state value, the covariance between beliefs regarding the trend and cyclical components is represented as $-\sigma_z^2$. The extent of confusion, denoted by σ_z^2, is influenced by two primary factors: the quality of signals (i.e., σ_e^2 and σ_ϵ^2) and the volatility of the state variables (i.e., σ_μ^2 and σ_x^2). First, forecasters receive private signals about each component in every period, which help them differentiate between the two. Consequently, more accurate signals decrease the level of confusion. Second, when the state innovations in the trend or cyclical component are more volatile, it becomes more difficult to identify each component, resulting in a higher level of confusion. Intuitively, the confusion is upper bounded by the uncertainty in either the trend or cyclical beliefs.

[8]Consider a special case nested in Equation (10). When the trend is stable (i.e., $\sigma_\mu^2 = 0$), forecasters can predict the trend component perfectly. Therefore, the error term in their beliefs regarding the trend component is zero. In this scenario, both the variance of the belief regarding the trend component (Var^T) and the covariance ($\widetilde{\text{COV}}$) would also be zero. As a result, the separation error in this case would be zero.

4 Forecasts over Horizon: Main Results

4.1 Covariance of Beliefs

The key difference between our benchmark model and the special case is that forecasters jointly update their beliefs regarding the two components. As a result, their beliefs about these two components are correlated, even when they are, in fact, independent. In this section, we analyze the covariance between forecasters' beliefs regarding trends and cycles after they have observed their private signals.

The covariance between forecasters' beliefs about the trend and cyclical components, captured by $\widetilde{\text{COV}}$ in Equation (9), is a crucial element of our model. This covariance depends on the volatility of the two components as well as the persistence of the cyclical component. Proposition 1 provides a detailed characterization of how these factors determine the sign and magnitude of the covariance of beliefs.

Proposition 1. *(i) The magnitude of the covariance between the trend and cyclical beliefs $|\widetilde{COV}|$ first increases and then decreases in the variance of trend innovations σ_μ^2; and it is zero when $\sigma_\mu^2 = 0$ and converges to zero when σ_μ^2 goes to ∞. (ii) The magnitude of the covariance increases with the persistence of the cyclical component (ρ). In particular, when $\rho = 0$, $\widetilde{COV} = 0$.*

To understand part (i), recall the covariance is characterized by $\widetilde{\text{COV}} = -\rho\sigma_\epsilon^2\sigma_e^2\sigma_z^2/\Omega$. As the variance of trend innovations (σ_μ^2) increases, two effects emerge. Firstly, Lemma 4 has shown that forecaster i's confusion, represented by σ_z^2, increases. Secondly, forecaster i's uncertainty about the state, represented by Ω, also increases. When the variance of trend innovations remains relatively small, the increase in confusion (σ_z^2) dominates. Conversely, when it is relatively large, the increase in overall variance (Ω) dominates.

Consider the following polar cases. When the trend is stable (i.e., $\sigma_\mu^2 = 0$), there is no confusion (i.e., $\sigma_z^2 = 0$). Therefore, the covariance is zero. When the trend innovation is very large (i.e., $\sigma_\mu^2 \to \infty$), forecaster i's uncertainty about the state is also very large (i.e., $\Omega \to \infty$), the confusion mechanism becomes irrelevant, and the covariance converges to zero too.

To understand part (ii), we first examine an extreme case where the persistence of the cyclical component is zero (i.e., $\rho = 0$). That is, the cyclical component becomes purely transitory, and our model reduces to a standard signal extraction problem. Consequently, signals regarding the cyclical components offer information solely about the cyclical components, which are uninformative for the trend components. Therefore, the covariance of beliefs regarding the two components is rendered to be zero. As the persistence (ρ) of the cyclical component increases, signals regarding the cyclical components become more valuable for revising trend beliefs, giving rise to a larger

covariance in magnitude.

4.2 Covariance between changes of long-run forecasts and cyclical forecasts

In this section, we examine the model's prediction for the covariance between changes in long-run and cyclical forecasts, which can be constructed from the data. Interestingly, we can relate the observable covariance in the data to the unobservable covariance between trend and cyclical beliefs in the model. We show the necessary and sufficient conditions under which our model can produce either a positive or negative covariance between changes in long-run and cyclical forecasts, and that the magnitude of the covariance decreases as the horizon h increases.

We begin our analysis by decomposing both the changes in the long-run forecasts and the cyclical forecasts. The changes in long-run forecasts is captured by changes in the forecasts for $h = 3Y$ periods ahead, which can be rewritten by:

$$F_{i,t}y_{t+3Y} - F_{i,t-1}y_{t-1+3Y} = (\mu^i_{1,t} - \mu^i_{1,t-1}) + \rho^{3Y}(x^i_{1,t} - x^i_{1,t-1}).$$

The changes in the long-run forecasts therefore reflect one's belief updates both in trend component (i.e., $\mu^i_{1,t} - \mu^i_{1,t-1}$) and cyclical component (i.e., $x^i_{1,t} - x^i_{1,t-1}$). On the other hand, the changes in the cyclical forecasts consist only the belief changes regarding the cyclical component:

$$Cyc^h_{i,t} - Cyc^h_{i,t-1} = (\rho^h - \rho^{3Y})(x^i_{1,t} - x^i_{1,t-1}). \tag{12}$$

The covariance between the changes in the long-run forecasts and cyclical forecasts can be written as follows:

$$\begin{aligned} COV^h_F &= cov(F_{i,t}y_{t+3Y} - F_{i,t-1}y_{t-1+3Y}, Cyc^h_{i,t} - Cyc^h_{i,t-1}) \\ &= \underbrace{(\rho^h - \rho^{3Y})}_{(+)} \underbrace{\left\{\widetilde{\text{COV}} + \rho^{3Y}\text{Var}^C\right\}}_{(+)\ or\ (-)}. \end{aligned} \tag{13}$$

The covariance COV^h_F can be positive or negative. For example, when a forecaster receives a signal indicating a stronger-than-expected cyclical component in the current period, she tends to revise the cyclical forecasts upwards. That is, $Cyc^h_{i,t} - Cyc^h_{i,t-1} > 0$. However, she can revise the long-term forecast either upwards ($F_{i,t}y_{t+3Y} - F_{i,t-1}y_{t-1+3Y} > 0$) or downwards ($F_{i,t}y_{t+3Y} - F_{i,t-1}y_{t-1+3Y} < 0$).

On the one hand, since the long-term forecast is partially driven by cyclical components, she may revise it upwards too. On the other hand, because the cyclical component is persistent, she revises her belief about the previous period's cyclical component upwards. This revision leads her to adjust her belief about the previous period's trend component downwards. This mechanism is shown in Section 3.2 (see Equation 9).

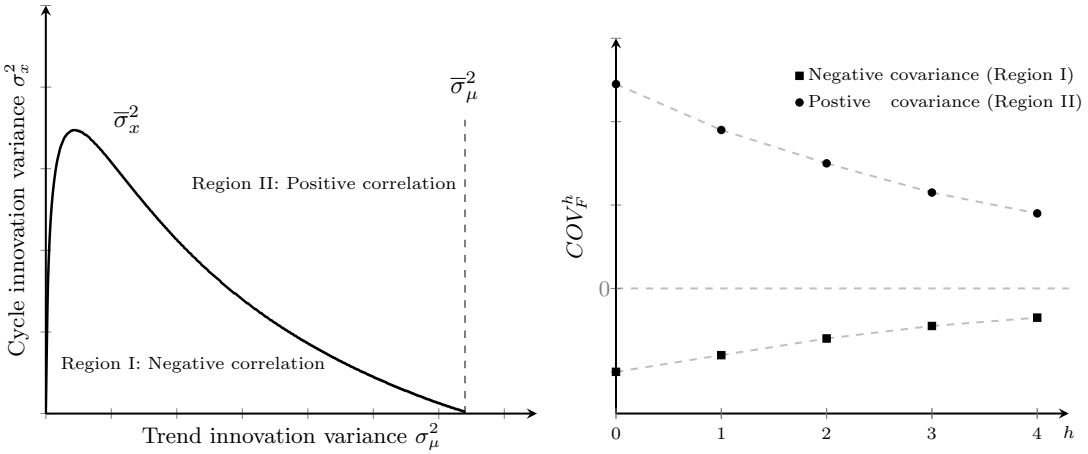

Figure 4. *The sign and the magnitude of the covariance between changes in the long-run forecasts and cyclical forecasts. Figure 4(a) demonstrates the sign of the COV_F^h. For a pair of state innovation $(\sigma_\mu^2, \sigma_x^2)$, the model predicts a negative covariance, if it lies inside Region I and a positive covariance if it lies in Region II. Figure 4(b) plots the COV_F^h at horizon $h = 0, 1, 2, 3, 4$. The figure shows that the magnitude of COV_F^h is always decreasing in h.*

It would suppress the estimate of trend component of the current period, causing a downward adjustment of the long-term forecasts.

The covariance term can be further decomposed into two parts, as shown in the second line of Equation (13). The first term, $(\rho^h - \rho^{3Y})$, is always positive and its magnitude depends on the forecast horizon h used to construct the cyclical forecasts. It decreases as the horizon h increases. When the cyclical forecast is constructed using the nowcast (i.e., $h = 0$), the first term reaches its largest value. As h approaches three years (i.e., $h = 3Y$), the first term goes to zero.

The second term can be either positive or negative. It consists of the covariance between trend and cyclical beliefs (i.e., $\widetilde{\text{COV}}$), and the variance of the cyclical belief (i.e., Var^{C}), each corresponding to one of the two mechanisms discussed earlier. Proposition 2 presents the necessary and sufficient conditions for the sum of the two terms to be negative.

Proposition 2. *There exists a threshold $\overline{\sigma}_\mu^2$ for the variance of the trend component innovation, such that:*
(i) for any $\sigma_\mu^2 \in [\overline{\sigma}_\mu^2, +\infty)$, COV_F^h is positive;
(ii) for any $\sigma_\mu^2 \in (0, \overline{\sigma}_\mu^2)$, there exists a threshold $\overline{\sigma}_x^2$ such that COV_F^h is negative if and only if $\sigma_x^2 < \overline{\sigma}_x^2$; and it is positive, otherwise;
(iii) and the magnitude of COV_F^h is decreasing as the horizon h increases.

Figure 4 illustrates how the sign and the magnitude of COV_F^h change, which is characterized by Proposition 2. Figure 4(a) demonstrates the sign of COV_F^h as the vari-

ance of the trend and cyclical innovation varies. For a pair of signal quality (captured by σ_ϵ^2 and σ_e^2), the model predicts a negative covariance when the trend component is moderately volatile, and the cyclical component is not excessively volatile.

As shown in Equation (13), the changes in long-run forecasts and cyclical forecasts exhibit a negative covariance when $\widetilde{\text{COV}}$ dominates. As shown in Proposition 1, this scenario occurs when the trend component is neither too stable nor too volatile. That explains item (i) in this proposition.

In addition, as the variance of the cyclical innovation (i.e., σ_x^2) increases, the variance of belief changes concerning the cyclical component (represented by the second term on the right-hand side of Equation (13)) also increases. If the cyclical component is too volatile, the confusion mechanism becomes less relevant. We show the existence of a threshold, $\overline{\sigma}_x^2$, for the volatility of cyclical components, such that changes in trend forecasts and cyclical forecasts exhibit a negative covariance when σ_x^2 is lower than this threshold. This explains item (ii) in this proposition.

Figure 4(b) shows that the magnitude of COV_F^h decreases as the forecast horizon increases. As Equation (12) shows, as h increases, changes in cyclical forecasts correspond to a smaller proportion of cyclical updates. That is, $(\rho^h - \rho^{3Y})$ decreases in h. Therefore, the magnitude of the covariance decreases and converges to zero as the forecast horizon h increases. That explains item (iii) in this proposition.

4.3 Forecast dispersion

We proceed to examine the prediction of our model regarding the relationship between the forecast dispersion and the forecast horizon. In our model, the forecast dispersion can either increase or decrease as the forecast horizon becomes longer. Proposition 3 characterizes the necessary and sufficient conditions for the forecast dispersion to increase or decrease over the forecast horizon.

To expound the mechanism, we decompose the dispersion of forecasts across forecasters for any horizon into three components: the variance arising from heterogeneous beliefs about the trend component, the cyclical component, and their covariance. To be specific, the forecast dispersion is given by:

$$E[(F_{i,t}y_{t+h} - \overline{E}[F_{i,t}y_{t+h}])^2] = \rho^{2h}\text{Var}^C\phi^C + \text{Var}^T\phi^T + 2\rho^h\widetilde{\text{COV}}\phi^{COV}, \tag{14}$$

where $0 < \phi^C < 1$, $0 < \phi^T < 1$ and $0 < \phi^{COV} < 1$ are positive scalars, whose expressions are collected in the proof of Proposition 3. Note that $\overline{E}[\cdot]$ is the mean forecast across all forecasters.

Figure 5 illustrates how each part changes as the forecast horizon extends. Figure 5(a) shows that the variance from heterogeneous beliefs about the cyclical component decreases when the forecast horizon extends. This reduction occurs because

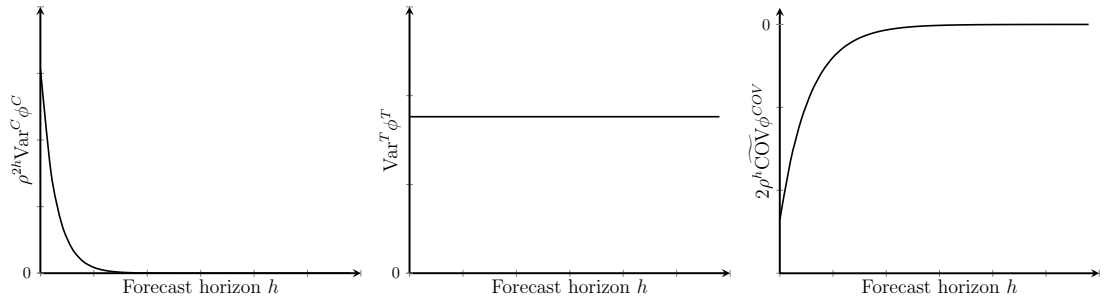

(a) Cycle beliefs (b) Trend beliefs (c) Covariance term

Figure 5. *Dispersion decomposition as the horizon extends. Note: This figure shows how each part of the dispersion changes as the forecast horizon extends.*

the cyclical component's influence diminishes in longer-term forecasts. Figure 5(b) demonstrates that the variance due to heterogeneous beliefs about the trend component remains constant across all horizons. This is expected, as the trend component's influence is consistent regardless of the forecast horizon. The behavior of these two components over different horizons aligns with what is observed in the special case (see section 4.4).

Figure 5(c) depicts the covariance term. Its magnitude decreases as the forecast horizon extends, due to the diminished importance of the cyclical component over longer horizons. This feature, though intuitive, is crucial for understanding our model's predictions. On the one hand, the covariance term is negative, reducing overall forecast dispersion across forecasters for any horizon. On the other hand, as the forecast horizon extends, the impact of the covariance term diminishes, leading to a force that drives up the forecast dispersion.

The change in forecast dispersion over a longer horizon is determined by the relative strength of two forces: the diminishing force from dispersion due to heterogeneous beliefs about the cyclical component, and the increasing force from the covariance term. Interestingly, in this model, forecast dispersion must increase with the forecast horizon when h is large enough. The dispersion of cyclical beliefs converges to zero more rapidly as the forecast horizon extends than the covariance between trend and cyclical beliefs. This is evident from Equation (14): ρ^{2h} converges to zero more quickly than ρ^h. Therefore, when the forecast horizon is sufficiently long, the increasing force of the covariance becomes dominant, leading to greater dispersion. Proposition 3 fully characterizes this property.

Proposition 3. *The dispersion of forecasts across forecasters is strictly increasing in the fore-*

cast horizon h, if and only if:

$$h > \underline{h} = \underbrace{\frac{1}{\ln \rho}}_{-} \underbrace{\ln \frac{-\widetilde{COV}}{Var^C} \frac{\phi^{COV}}{\phi^C} W}_{- \quad or \quad +}; \tag{15}$$

where $W < 1$ is a positive scalar given by $E[(z_{i,t} - E[z_{i,t}])^2]/\sigma_z^2$ and $\ln \rho < 0$.

When the threshold is negative ($\underline{h} \leq 0$), forecast dispersion always increases over the forecast horizon. This scenario occurs when the variance of the trend innovation is moderate. As shown in Proposition 1, in such cases, the impact of the covariance between trend and cyclical beliefs (i.e., $\widetilde{COV}$) is greatest.

Conversely, when the threshold value on the right-hand side of Equation (15) approaches infinity ($\underline{h} \to \infty$), forecast dispersion always decreases over the forecast horizon. This scenario occurs in the special case described in section 4.4, where forecasters can perfectly differentiate between trend and cyclical components, resulting in a covariance term of zero.

4.4 Special Cases and Generalization

In this section, we highlight the inability to perfectly separate multiple persistent components is the key to generate the this set of model predictions which are consistent with the documented facts. Towards this end, we examine two special cases and one generalization of our model. In the first special case, we allow forecasters to perfectly separate the trend and cyclical components. In the second special case, we consider a situation where the cyclical component is transitory. In the generalization, we relax the assumption that the trend component follows a random walk.

First, we consider a special case in which forecasters can perfectly separate the two components. In this scenario, we assume that forecasters directly observe the trend component at the end of each period. Consequently, forecasters can perfectly disentangle the two components, and the separation error becomes zero (i.e., $\sigma_z^2 = 0$). Without any confusion between components, forecasters update their beliefs regarding the trend and cyclical components independently. Recall Equation (9), this independence implies that the covariance between beliefs regarding the trend and cyclical components is zero, i.e., $\widetilde{\text{COV}} = 0$.

When the covariance between the beliefs regarding the two components becomes zero, the model predicts that the covariance between the changes in the long-run and cyclical forecasts should be non-negative, and the forecast dispersion across forecasters must be decreasing as the forecast horizon extends. On the one hand, the changes in the long-run forecast reflect updating in both trend and cyclical components, while the changes in the cyclical forecast reflect only updating in the cyclical component. Given that trend and cyclical beliefs are independent, the covariance between the

changes in the long-run and cyclical forecasts must be positive in this special case.

On the other hand, forecast dispersion across forecasters stems from their disagreement about both trend and cyclical components. As the forecast horizon extends, the cyclical belief becomes less important, and the disagreement regarding the cyclical component also becomes less important. As a result, the forecast dispersion decreases as the forecast horizon extends. All the detailed specifications are provided in Appendix B.2.

The second special case examines a scenario in which the cyclical component is transitory (i.e., $\rho = 0$), while maintaining all other model specifications unchanged. This coincides with the setting that has been widely studied in signal extraction problems. In this special case, since households cannot directly observe the value of each component, forecasters still cannot perfectly disentangle the two components, resulting in non-zero separation error. However, because the cyclical signal observed in the current period contains no information about the cyclical component in the last period, forecasters would not use the cyclical signal to update their beliefs regarding the trend component. As a result, recall Equation (9), the covariance between the beliefs regarding the trend and cyclical components is zero, i.e., $\widetilde{\text{COV}} = 0$. Therefore, the model's predictions about the covariance between the changes in the long-run and cyclical forecasts, and the forecast dispersion across horizons, are analogous to the first special case.

Finally, we also generalize this model by relaxing the assumption that the trend component follows a random walk, allowing it to be persistent instead. We show that under this specification, the key mechanism of our model framework is maintained: the covariance between forecasters' beliefs regarding the trend and cyclical components can be negative. This highlights that our key mechanism stems from the inability to separate multiple persistent components, rather than from the random walk assumption for the trend component. In Appendix B.2, we provide characterization and proofs for this generalization.

5 Model Validation: Explicit Inflation Targeting

In the previous sections, we fully characterized our model and demonstrated how it generates various qualitative empirical patterns depending on the parameter space. Specifically, our model predicts that the covariance between changes in long-run forecasts and cyclical forecasts can be either positive or negative under certain conditions of the data generating process. Similarly, forecast dispersion can either increase or decrease over the forecast horizon depending on specific properties of the underlying processes.

To validate these theoretical predictions, we leverage a policy shock: a policy change that altered the underlying parameters of the data generating process. By examining

whether the observed changes in forecasting patterns following this policy shift align with our model's predictions, we can assess the validity of our model mechanism.

Specifically, we examine the effects of the introduction of explicit inflation targeting in the United States in 2012. This new approach to monetary policy implementation began with an announcement on January 25th by Ben Bernanke, the Chairman of the U.S. Federal Reserve, who set a specific inflation target of 2%. Prior to this policy change, the United States did not have an explicit inflation target, relying instead on regularly announced desired target ranges for inflation.[9, 10]

5.1 Method

Through the lens of our model, the implication of this policy for forecasters is that the underlying data generation process for inflation could undergo changes which would necessitate changes in forecasting behaviors. To quantify the underlying changes caused by the policy implementation, we begin by dividing the sample into two subsamples: the period before 2012 and the period after. We then structurally estimate the model using moments obtained from both the pre- and post-2012 sub-samples. We then assess the estimated changes in the data generation process and examine how they impact the empirical patterns of forecasts quantitatively. While all the details of the estimation are provided in Appendix A.6, we summarize the estimation procedures below. Note that we use the ten-year-ahead forecasts of the inflation rate in the SPF as the long-term forecasts because the SPF does not provide three-year-ahead forecasts for inflation. The ten-year-ahead forecast data have been available since 1991Q4.

Our model can be fully specified by five parameters: $\{\rho, \sigma_\mu^2, \sigma_x^2, \sigma_\epsilon^2, \sigma_e^2\}$. The first three parameters are related to the data generating process, while the last two capture the precision of the signals. To structurally estimate the values of these parameters, we follow the approach of Chernozhukov and Hong (2003) and compute Laplace-type estimators (LTE) using a Markov Chain Monte Carlo method. To identify changes in the underlying parameters, we estimate them for each subsample period.

We estimated the model parameters by targeting the forecast variance across different horizons in each subsample period. We then used the estimated model to simulate

[9]Before the era of the Greenspan Fed, the Federal Reserve operated under a stop-and-go policy without a specific inflation target. Starting in 1992, the Greenspan Fed aimed to maintain low long-term inflation rates (see Goodfriend 2004 for a comprehensive review). From the 1990s until the Great Recession, there was a consensus among market participants and FOMC members that the optimal inflation target would fall between 1% and 2%. However, there was no explicit inflation target (Shapiro and Wilson 2019). In January 2012, the FOMC announced a target of 2% for the inflation rate, marking the first time in its history that it adopted an explicit inflation-targeting approach.

[10]While this policy shift was the most significant change in monetary policy in 2012 and likely consequential for inflation expectations, we acknowledge that multiple factors could have contributed to the structural changes in inflation forecasting patterns observed around the 2010s. Therefore, the timing coincidence between inflation targeting adoption and changes in inflation expectations patterns should be interpreted as correlation rather than a causal relationship. This correlation serves as a useful validation test for our model mechanism–a necessary but not sufficient condition to satisfy.

Table 2. *Estimated Model Parameters*

	Parameter Estimation					
	Pre-2012			Post-2012		
	Mean	90 HPDI	95 HPDI	Mean	90 HPDI	95 HPDI
σ_μ^2	1.14	(0.96,1.38)	(0.91,1.38)	0.84	(0.66,1.08)	(0.61,1.08)
σ_x^2	2.57	(2.41,2.67)	(2.43,2.75)	2.60	(2.37,2.76)	(2.40,2.88)
σ_ϵ^2	0.78	(0.62,0.89)	(0.61,0.95)	0.72	(0.48,0.89)	(0.47,0.97)
σ_e^2	1.62	(1.47,1.76)	(1.47,1.77)	1.54	(1.31,1.74)	(1.30,1.76)
ρ	0.84	(0.73,0.94)	(0.74,0.97)	0.64	(0.53,0.76)	(0.53,0.79)

Note: This table presents the estimated parameter values for the pre-2012 and post-2012 periods. We provide the mean values, as well as the 90% and 95% Highest Posterior Density Intervals (HPDI).

data and examine the covariance patterns, which were not targeted in the estimation. This approach allowed us to assess the model's quantitative predictions about the effects of the policy shift in 2012.

To be concrete, we compute the across quarters average variances of forecasts for different horizons, specifically for $h = 0, 1, 2, 3, 4$, using the subsamples before and after 2012. These variances will be treated as the target moments in our estimation and denoted as $\hat{m}$. Furthermore, we construct the model counterpart of $\hat{m}$ and define the distance between the two as follows:

$$\Lambda(\Theta) = [m(\Theta) - \hat{m}]' \hat{W} [m(\Theta) - \hat{m}], \tag{16}$$

where $\hat{W}$ is the weighting matrix, where the diagonal elements represent the precision of the moments $\hat{m}$. We solve for the parameter values (Θ) to minimize the constructed distance, that is, finding the set of parameter values that best matches the forecast variance at each forecast horizon.

5.2 Results

The estimated parameters for each subsample are reported in Table 2 together with the 90% and 95% high posterior density interval (HPDI). A comparison of the two sets of estimated parameters reveals that there are minimal changes in the innovations in cycles variance (i.e., σ_x^2) and the precision of signals on trends and cycles (i.e., σ_ϵ^2 and σ_e^2) following the policy change in 2012. This indicates that this set of parameters remain relatively stable before and after the policy change.

There are two noteworthy changes. First, there is a sizable decrease in the variance of trend innovation (i.e., σ_μ^2). Before the policy change, the estimated variance was 1.14. After the policy change, it dropped to 0.84. This suggests that the trend is

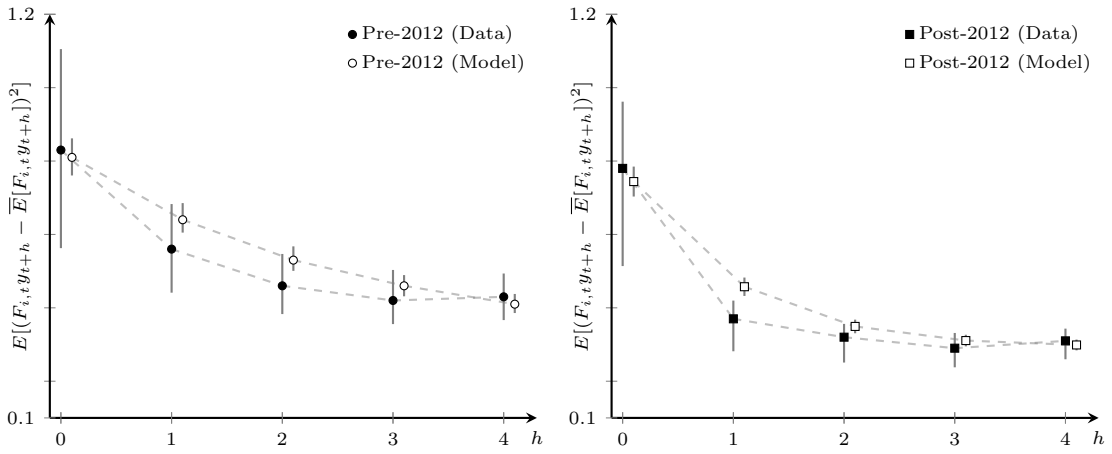

(a) Forecast variance before 2012 (b) Forecast variance after 2012

Figure 6. *Forecast variance over horizon for the subsamples before and after 2012. Black dots represent results from SPF data, while white dots depict simulated data. Figure 6(a) shows forecast variance before 2012, and Figure 6(b) illustrates it after 2012. The gray solid line marks the 95% confidence interval using the bootstrap method. Our model fits the data closely in both sub-samples. The pre-2012 period spans from 1990Q1 to 2011Q4, and the post-2012 period from 2012Q1 to 2019Q4.*

more stable after the policy implementation, consistent with the policy goal of providing a specific long-run target. Second, the persistence of the cyclical component (i.e., ρ) decreases. Before the policy change, the estimated persistence of the cyclical component was 0.84, aligning with previous literature. For instance, Carvalho et al. (2023) estimated a value of $\rho = 0.87$. After the policy change, the estimated persistence dropped to 0.64, indicating that short-term fluctuations have become less persistent. The observed change in the estimated persistence of the cyclical component is intuitive. Following the policy change, the central bank would respond more aggressively to short-term deviations from the long-term target. Consequently, the persistence of the cyclical component would decrease.

Next, we investigate whether the estimated model can reproduce the set of findings documented in Section 2 concerning inflation forecasts before and after 2012. First, we examine the forecast variance across various forecast horizons, which were targeted moments in the estimation. Figure 6 displays the forecast variance of the SPF data and the simulated data before and after 2012. The black dots represent results obtained using the SPF data, while the white dots represent the simulated data. The gray solid line corresponds to the 95% confidence interval using the bootstrap method. In both sub-samples, the simulated models closely fit the empirical data.

In the SPF data, a notable difference between the two sample periods is observed: the forecast variance declines more rapidly as the forecast horizon extends in the post-2012 sub-sample compared to the pre-2012 period. Specifically, in the pre-2012 sub-sample, the forecast variance decreases by 32.5%, from 0.833 at the now-cast ($h = 0$) to

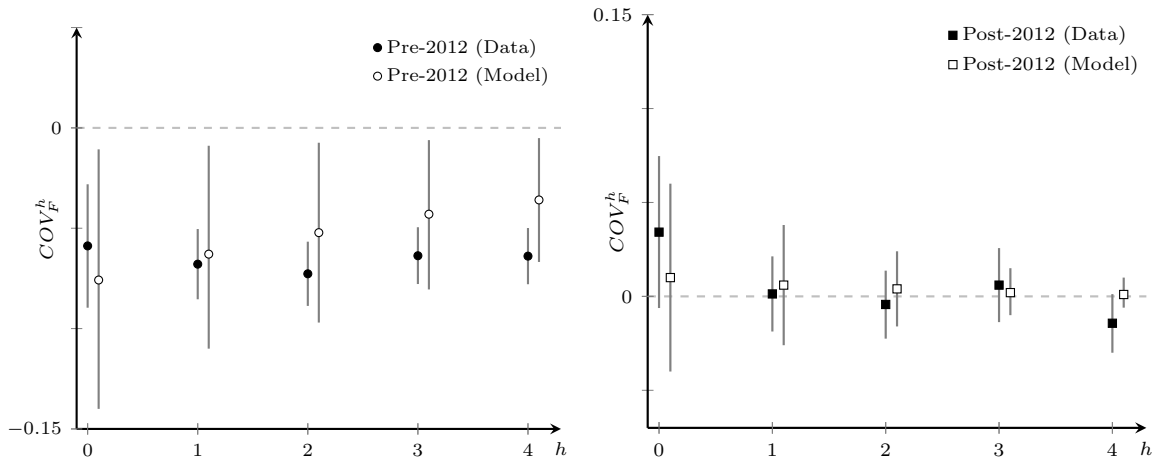

(a) COV_F^h before 2012 (b) COV_F^h after 2012

Figure 7. *The estimated COV_F^h for the subsamples before and after 2012. Black dots represent the results obtained using SPF data, while white dots represent the simulated data. In Figures 7(a) and 7(b), we observe that the covariance is negative before 2012 and positive or close to zero after 2012. The sample period for the pre-2012 sub-sample ranges from 1990Q1 to 2011Q4, while the post-2012 sub-sample spans from 2012Q1 to 2019Q4.*

0.562 for forecasts one quarter ahead. In contrast, the post-2012 subsample exhibits a much sharper decline of 52.5%, with the variance dropping from 0.737 at the now-cast to 0.350 for one-quarter-ahead forecasts.

The change in empirical patterns across the two periods aligns qualitatively with our model's predictions. According to Proposition 1, when the trend component becomes more stable (i.e., σ_μ^2 decreases) and the cyclical component becomes less persistent (i.e., ρ decreases), the magnitude of the negative covariance between trend and cyclical beliefs decreases. This is because, as the trend component becomes more stable, forecasters can better separate the trend from the cycle; and as the persistence of the cyclical component decreases, new information about the cyclical component becomes less relevant for updating the trend component. As a result, the force from the confusion mechanism plays a less important role, and the overall forecast dispersion decreases at a faster rate.

Second, we examine the covariance between changes in the long-run forecasts and cyclical forecasts in both sub-samples. It is important to stress that this covariance was not a targeted moment in the estimation.

The empirical results from the SPF data reveal an intriguing shift in forecasting behavior. Figure 7(a) shows a significant negative covariance between changes in long-run forecasts and cyclical forecasts in the pre-2012 sub-sample. In constrast, Figure 7(b) illustrates that this covariance becomes positive and insignificant in the post-2012 sub-sample.

This reversal in sign following the implementation of inflation targeting aligns with our model's prediction. As previously discussed, when the trend component becomes more stable and the cyclical component less persistent, the confusion mechanism's effect weakens. Consequently, the empirical covariance patterns should more closely match those predicted by the observable-trend model in section 4.4, where the confusion mechanism is absent. Our model predicts that after the policy change, the covariance between changes in trend forecasts and changes in cyclical forecasts is more likely to be non-negative.

Qualitatively, the estimated results from the simulated data closely align with the empirical results using the SPF data in both subsamples. Figure 7 contrasts the results in the SPF data with those from the simulation data. Despite its simplicity and limited number of parameters, our model effectively captures the shift in forecasting patterns following the policy change and quantitatively reproduces the changes observed in the actual data.[11]

6 Model Application: Revisiting FE-FR Regressions

In this section, we revisit the Forecast Error-Forecast Revision (FE-FR) regression approach pioneered by Coibion and Gorodnichenko (2015) at the consensus level and Bordalo et al. (2020) at the individual level. While these seminal works typically assume a single, stationary AR(1) process, our framework incorporates potentially non-stationary trend and cyclical components that forecasters cannot perfectly distinguish. We examine the robustness of FE-FR regressions within this enriched environment and reveal new insights that emerge when accounting for trend-cycle confusion.

6.1 FE-FR Regressions at Consensus Level

Coibion and Gorodnichenko (2015) quantify information rigidity using a consensus-level regression that relates forecast errors to forecast revisions:

$$\underbrace{y_t - F_t y_t}_{Forecast\ Error} = c + \beta_{CG}(\underbrace{F_t y_t - F_{t-1} y_t}_{Forecast\ Revision}) + v_t, \tag{17}$$

where $F_t y_t$ represents the consensus forecast of y_t across forecasters. Their key finding is that β_{CG} is positive across various macroeconomic variables, indicating that consensus forecast errors are systematically predictable by forecast revisions. For stationary processes (including AR(1)), they demonstrate that this "CG coefficient"directly measures the degree of information friction within the noisy information framework.

[11] We also estimated parameters for real GDP growth and unemployment using identical procedures. Results reveal two key differences from inflation: (1) forecasters perceive substantially less volatile cyclical components for these variables, moderating cyclical disagreement, and (2) signal quality is notably lower, hindering trend-cycle separation. These parameter differences explain the contrasting forecast dispersion patterns documented in Table 1, where dispersion increases with horizon for GDP and unemployment but decreases for inflation.

In our framework, the data generation process includes non-stationary trend components, which forecasters cannot perfectly distinguish from cyclical components. Proposition 4 re-examines this approach and investigates how the CG coefficient relates to the extent of underlying information frictions in this environment.

Proposition 4. *When y_t consists of both trend and cyclical components described by Equation (5), the CG coefficient β_{CG}^{Trend}, estimated using Equation (17), can be decomposed by:*

$$\begin{aligned}\beta_{CG}^{Trend} = & \underbrace{\frac{1-\boldsymbol{\kappa}_{11}}{\boldsymbol{\kappa}_{11}} + \frac{1-\boldsymbol{\kappa}_{22}}{\boldsymbol{\kappa}_{22}}}_{(+)\ Effect\ of\ noisy\ information} + \underbrace{\frac{\boldsymbol{\kappa}_{11}\boldsymbol{\kappa}_{12}(\boldsymbol{\kappa}_{21}-\boldsymbol{\kappa}_{22}) + \boldsymbol{\kappa}_{22}\boldsymbol{\kappa}_{21}(\boldsymbol{\kappa}_{12}-\boldsymbol{\kappa}_{11})}{\boldsymbol{\kappa}_{11}\boldsymbol{\kappa}_{22}(\boldsymbol{\kappa}_{11}\boldsymbol{\kappa}_{22}-\boldsymbol{\kappa}_{12}\boldsymbol{\kappa}_{21})}}_{(+)\ Effect\ of\ confusing\ trends\ and\ cycles} \\ & \underbrace{- \boldsymbol{I}\boldsymbol{\kappa}^{-1}(\boldsymbol{I}-\boldsymbol{\kappa})\boldsymbol{I}' \frac{cov(F_t y_t - F_{t-1}y_t,\ F_{2,t-1}y_t - F_{t-1}y_t)}{var(F_t y_t - F_{t-1}y_t)}}_{(+)\ Effect\ of\ the\ second\ updating} \\ & > 0,\end{aligned} \tag{18}$$

where $\boldsymbol{I}$ is the identity matrix, $\boldsymbol{\kappa}$ is the Kalman gain matrix specified in Equation (8), and $\boldsymbol{\kappa}_{ij}$ represents the element at row i and column j of the Kalman gain matrix.

Proposition (4) implies that the estimated β_{CG}^{Trend} in this environment provides a lower bound for the extent of information friction. To understand, we start by characterizing the consensus forecast error as follows:

$$\underbrace{y_t - F_t y_t}_{Forecast\ Error} = \boldsymbol{I}\boldsymbol{\kappa}^{-1}(\boldsymbol{I}-\boldsymbol{\kappa})\boldsymbol{I}' \underbrace{(F_t y_t - F_{t-1}y_t)}_{Forecast\ Revision} - \boldsymbol{I}\boldsymbol{\kappa}^{-1}(\boldsymbol{I}-\boldsymbol{\kappa})\boldsymbol{I}' \underbrace{(F_{2,t-1}y_t - F_{t-1}y_t)}_{Effect\ of\ the\ second\ updating}, \tag{19}$$

where $F_{2,t-1}y_t$ is the mean forecast across forecasters after observing the actual state value y_{t-1}, i.e., $F_{2,t-1}y_t \equiv \overline{E}[\mu_{2,t-1}^i + \rho x_{2,t-1}^i]$. Note that in our model, forecasters update their beliefs twice each period. As a result, the prior belief of period t is $F_{2,t-1}y_t$, which is the posterior belief after observing y_{t-1} at the end of period $t-1$.

The information friction in this model comes from two sources: noisy information and confusion, which are embedded in the term $\boldsymbol{I}\boldsymbol{\kappa}^{-1}(\boldsymbol{I}-\boldsymbol{\kappa})\boldsymbol{I}'$ of Equation (19). The first term on the right-hand side of Equation (18) captures the former, representing a weighted average of the extent of information friction in the two components. Note that when the trends are stable (i.e., $\boldsymbol{\kappa}_{11} = 1$), this term reduces to $(1-\boldsymbol{\kappa}_{22})/\boldsymbol{\kappa}_{22}$, which is the CG coefficient β_{CG} characterized in Coibion and Gorodnichenko (2015).

The second term on the right-hand side of Equation (18) captures the impact of confusion. In our model, forecasters utilize the trend (cyclical) signal to update their beliefs about the cyclical (trend) component. For example, when forecasters observe a positive surprise from the trend signal (i.e., $s_{i,t}^{\mu} - \mu_{2,t-1}^i > 0$), they may interpret it partly as an indication of a strong trend innovation and partly as a lower trend component in the previous period. This leads to a situation that is observationally equivalent

to forecasters having noisier signals. This mechanism drives up the correlation between forecast revisions and forecast errors, explaining why the second term on the right-hand side of Equation (18) is positive. Note that if trends and cycles are perfectly observable (i.e., $\boldsymbol{\kappa}_{12} = \boldsymbol{\kappa}_{21} = 0$), this term reduces to zero.

The third term on the right-hand side of Equation (18) characterizes the effect of the second belief updating at the of period $t-1$ after forecasters observe the statistics y_{t-1}, which is embedded in the term $(F_{2,t-1}y_t - F_{t-1}y_t)$ in Equation (19). When y_{t-1} is observable, it is used to update the belief about y_t, and the posterior belief becomes $F_{2,t-1}y_t$. The observation of y_{t-1} affects both forecast revisions and forecast errors. For example, when y_{t-1} is larger, the updated forecast for y_t next period ($F_t y_t$) tends to be larger, resulting in a larger forecast revision $(F_t y_t - F_{t-1}y_t)$ and a smaller forecast error $(y_t - F_t y_t)$. This mechanism biases the coefficient downwards, explaining why the third term is negative.

Interestingly, when y_{t-1} is not observable, the posterior belief about y_t in period $t-1$ would be $F_{t-1}y_t$. There would be no second updating and the term $(F_{2,t-1}y_t - F_{t-1}y_t)$ in Equation (19) would be zero. In this case, forecasters would update their beliefs about trend and cyclical components independently, leading to no confusion between the two. That is, $\boldsymbol{\kappa}_{12} = \boldsymbol{\kappa}_{21} = 0$. Therefore, the second term on the right-hand side of Equation (18) reduces to zero too. Consequently, the CG coefficient would correspond exactly to the extent of noisy information.

Because the third term on the right-hand side of Equation (18) is negative, the actual extent of information friction can be even larger than the coefficient β_{CG}^{Trend} suggests. In other words, the CG coefficient provides a lower bound on the level of information friction. This finding suggests that the CG specification remains a robust measure for uncovering information friction stemming from noisy information, even within our framework.

6.2 FE-FR Regressions at Individual Level

Bordalo et al. (2020) document forecaster overreaction to new information through individual-level FE-FR regressions, a finding later extended by Afrouzi et al. (2023), who show this overreaction can be larger at longer horizons. We revisit these empirical patterns and demonstrate how a minimal extension of our benchmark model can deliver a pattern consistent with this empirical findings.

The individual-level FE-FR regression from Bordalo et al. (2020) is specified as:

$$y_{t+h} - F_{i,t}y_{t+h} = \alpha + \beta_{ind}^{h}(F_{i,t}y_{t+h} - F_{i,t-1}y_{t+h}) + u_{i,t}, \tag{20}$$

where the left term represents forecaster i's forecast error at horizon h, and the term in parentheses captures their forecast revision. Under rational expectations, β_{ind}^{h} should equal zero, as forecast errors should be unpredictable using information in the fore-

caster's set. A negative coefficient indicates overreaction to information, while a positive one signals underreaction.

To study the overreaction pattern in our framework, we first extend the benchmark model to introduce overconfidence, where forecasters subjectively believe that the variances of signal noise are smaller than their actual values (Broer and Kohlhas 2024). Specifically, we consider a scenario where forecasters perceive the signal variances of the trend component as $m\sigma_\epsilon^2$. When $m < 1$, it corresponds to the case where forecasters subjectively believe the trend signal is more precise than it actually is.

In a model where the state variable consists of a single component, as in Broer and Kohlhas (2024), the extent of overreaction remains constant across forecast horizons, i.e., the coefficient β_{ind}^h does not vary with h. In contrast, in our framework with multiple components, the extent of overreaction could be stronger in the long run under certain conditions. Proposition 5 summarizes this result.

Proposition 5. *When forecasters are sufficiently overconfident in the trend signal, there exists a unique cutoff σ_x^* such that if and only if $\sigma_x > \sigma_x^*$,*

$$\beta_{ind}^L < \beta_{ind}^S < 0,$$

where β_{ind}^S and β_{ind}^L represent coefficients for short-horizon ($h = 0$) and long-horizon (sufficiently large h) forecasts, respectively.

Proposition 5 states that when the cyclical component is volatile enough and forecasters are sufficiently overconfident, the model predicts a smaller coefficient for long-run forecasts than for short-run forecasts, indicating stronger overreaction in long-run forecasts. Intuitively, for long-run forecasts, β_{ind}^L primarily reflects the relationship between forecast error in the trend component and revision in trend belief, as the cyclical component becomes less relevant at longer horizons. When forecasters overweight trend signals in updating their beliefs, forecast errors and forecast revisions regarding the trend component become negatively correlated – a standard result in the overconfidence literature.

For short-run forecasts, β_{ind}^S incorporates both trend and cyclical components. Two opposing forces emerge.[12] The direct effect weakens the impact of trend overconfidence in short-run forecasts because forecast revisions now include cyclical component revisions not driven by overconfidence. This effect alone would make overreaction stronger in long-run forecasts.

[12]When forecasters are sufficiently overconfident, they rely heavily on trend signals when forming trend beliefs. The forecasters would not use the trend signal when updating their beliefs regarding the cyclical component since they subjectively believe they can separate the two components well. Consequently, any effect from the covariance between cyclical revision and trend forecast error becomes negligible.

However, a countervailing separation effect exists in our model: overconfident forecasters believe they can separate trend and cyclical components better than they actually can. By underestimating the separation error variance, they overweight their cyclical prior beliefs. This causes stronger correlation between cyclical forecast errors and overall forecast revisions in the short run, leading to stronger overreaction in short-run forecasts. This effect makes overreaction stronger in short-run forecasts.

The balance between these opposing forces depends critically on cyclical component volatility. When the cyclical component is relatively stable, the direct effect weakens while the separation effect strengthens, making overreaction milder for long-run forecasts. Conversely, when cyclical volatility exceeds the threshold σ_x^*, forecasters rely less on the cyclical prior, leading to a weaker separation effect. In addition, the direct effect strengthens because cyclical components play a more important role in short-run forecasts. Therefore, the direct effect dominates, resulting in stronger overreaction for long-run forecasts compared to short-run forecasts – the pattern documented in empirical studies.

Our results in this section demonstrate that incorporating trend-cycle confusion into forecasting models yields important insights about horizon-dependent overreaction. By allowing forecasters to distinguish imperfectly between trend and cyclical components, even a minimal deviation from our framework generates stronger overreaction in long-horizon forecasts than in short-horizon forecasts. This mechanism offers a parsimonious alternative to models requiring additional cognitive limitations to generate similar patterns.

7 Conclusion

This paper introduces a framework where forecasters face rational confusion in distinguishing between trend and cyclical components of state variables. We show that this key feature accounts for a range of forecasting patterns at both individual and aggregate levels. Our quantitative validation examines the 2012 inflation targeting policy, demonstrating that resulting changes in empirical forecasting behavior align with our model's predictions. With this framework, we revisit the FE-FR regression approach proposed by Coibion and Gorodnichenko (2015) and Bordalo et al. (2020). We examine the robustness of these regressions at the consensus level and identify new insights arising from trend-cycle confusion at the individual level.

The applications of this framework extend beyond forecasting to any context where individuals must disentangle two persistent but imperfectly separable processes. Potential applications include investors separating sectoral from firm-specific earnings components and voters distinguishing between candidate quality and circumstantial factors. We leave the development of these broader applications to future work.

References

Afrouzi, H., S. Y. Kwon, A. Landier, Y. Ma, and D. Thesmar (2023). Overreaction in expectations: Evidence and theory. *The Quarterly Journal of Economics 138*(3), 1713–1764.

Almeida, H., M. Campello, and M. S. Weisbach (2004). The cash flow sensitivity of cash. *The Journal of Finance 59*(4), 1777–1804.

Andrade, P., R. K. Crump, S. Eusepi, and E. Moench (2016). Fundamental disagreement. *Journal of Monetary Economics 83*, 106–128.

Angeletos, G.-M. and Z. Huo (2021). Myopia and anchoring. *American Economic Review 111*(4), 1166–1200.

Antolin-Diaz, J., T. Drechsel, and I. Petrella (2017). Tracking the slowdown in long-run gdp growth. *Review of Economics and Statistics 99*(2), 343–356.

Blanchard, O. J. and L. H. Summers (1986). Hysteresis and the european unemployment problem. *NBER Macroeconomics Annual 1*, 15–78.

Bordalo, P., N. Gennaioli, Y. Ma, and A. Shleifer (2020). Overreaction in macroeconomic expectations. *American Economic Review 110*(9), 2748–2782.

Bostanci, G. and G. Ordoñez (2024). Business, liquidity, and information cycles.

Broer, T. and A. N. Kohlhas (2024). Forecaster (mis-) behavior. *Review of Economics and Statistics 106*(5), 1334–1351.

Carvalho, C., S. Eusepi, E. Moench, and B. Preston (2023). Anchored inflation expectations. *American Economic Journal: Macroeconomics 15*(1), 1–47.

Chen, H., X. Li, G. Pei, and Q. Xin (2024). Heterogeneous overreaction in expectation formation: Evidence and theory. *Journal of Economic Theory*, 105839.

Chernozhukov, V. and H. Hong (2003). An mcmc approach to classical estimation. *Journal of Econometrics 115*(2), 293–346.

Coibion, O. and Y. Gorodnichenko (2015). Information rigidity and the expectations formation process: A simple framework and new facts. *American Economic Review 105*(8), 2644–2678.

Collard, F., H. Dellas, and F. Smets (2009). Imperfect information and the business cycle. *Journal of Monetary Economics 56*, S38–S56.

Delle Monache, D., A. De Polis, and I. Petrella (2024). Modeling and forecasting macroeconomic downside risk. *Journal of Business & Economic Statistics 42*(3), 1010–1025.

Farmer, L. E., E. Nakamura, and J. Steinsson (2024). Learning about the long run. *Journal of Political Economy 132*(10), 3334–3377.

Fisher, J. D., L. Melosi, and S. Rast (2025). Long-run inflation expectations.

Folland, G. B. (2009). *Fourier analysis and its applications*, Volume 4. American Mathematical Soc.

Furlanetto, F., A. Lepetit, Ø. Robstad, J. Rubio-Ramírez, and P. Ulvedal (2025). Estimating hysteresis effects. *American Economic Journal: Macroeconomics 17*(1), 35–70.

Goodfriend, M. (2004). Inflation targeting in the united states? In *The inflation-targeting debate*, pp. 311–352. University of Chicago Press.

Huo, Z., M. Pedroni, and G. Pei (2024). Bias and sensitivity under ambiguity. *American Economic Review 114*(12), 4091–4133.

Kohlhas, A. N. and A. Walther (2021). Asymmetric attention. *American Economic Review 111*(9), 2879–2925.

Lahiri, K. and X. Sheng (2008). Evolution of forecast disagreement in a bayesian learning model. *Journal of Econometrics 144*(2), 325–340.

Lorenzoni, G. (2009). A theory of demand shocks. *American Economic Review 99*(5), 2050–2084.

Lucas, R. E. and E. C. Prescott (1978). Equilibrium search and unemployment. In *Uncertainty in economics*, pp. 515–540.

Lucas, R. E. (1972). Expectations and the neutrality of money. *Journal of economic theory 4*(2), 103–124.

Muth, J. F. (1960). Optimal properties of exponentially weighted forecasts. *Journal of the American Statistical Association 55*(290), 299–306.

Patton, A. J. and A. Timmermann (2010). Why do forecasters disagree? lessons from the term structure of cross-sectional dispersion. *Journal of Monetary Economics 57*(7), 803–820.

Rozsypal, F. and K. Schlafmann (2023). Overpersistence bias in individual income expectations and its aggregate implications. *American Economic Journal: Macroeconomics 15*(4), 331–371.

Shapiro, A. and D. J. Wilson (2019). The evolution of the fomc's explicit inflation target. *Evolution 2019*, 12.

Stock, J. H. and M. W. Watson (1998). Median unbiased estimation of coefficient variance in a time-varying parameter model. *Journal of the American Statistical Association 93*(441), 349–358.

Wang, T. and C. Hou (2024). Uncovering subjective models from survey expectations. *Available at SSRN 3728884*.

Xie, S. (2023). An estimated model of household inflation expectations: Information frictions and implications. *Review of Economics and Statistics*, 1–45.

Appendix

A Data and Robustness Tests

A.1 Sample periods and variable definition

The data used in this paper are from the Survey of Professional Forecasters (SPF). Table 3 provides a list of the periods for which each forecast variable is available.

Table 3. *Summary of sample periods*

Summary of sample periods	
Forecast Variable	Sample periods
Panel A. Short-term Forecasts.	
Nominal GDP	1968Q4 - 2019Q4
Real GDP	1968Q4 - 2019Q4
GDP price index inflation	1968Q4 - 2019Q4
Real consumption	1981Q3 - 2019Q4
Industrial production	1968Q4 - 2019Q4
Real nonresidential investment	1981Q3 - 2019Q4
Real residential investment	1981Q3 - 2019Q4
Real federal government consumption	1981Q3 - 2019Q4
Real state and local government consumption	1981Q3 - 2019Q4
Housing start	1968Q4 - 2019Q4
Unemployment	1968Q4 - 2019Q4
Inflation (CPI)	1981Q3 - 2019Q4
Three-month Treasury rate	1981Q3 - 2019Q4
Ten-year Treasury rate	1992Q1 - 2019Q4
Panel B. Long-term Forecasts.	
Three-year ahead Real GDP	2009Q2-2019Q4
Three-year ahead unemployment	2009Q2-2019Q4
Ten-year ahead inflation (CPI)	1991Q3-2019Q4
Ten-year ahead Real GDP	1992Q1-2019Q1; first quarter only
Natural rate of unemployment	1996Q3-2019Q3; third quarter only

Following Bordalo et al. (2020), we convert macroeconomic variables to annual growth rates. For variables that are already presented as rates, we use the original data directly.

Variables changed to the annual growth rate include nominal GDP (NGDP), real GDP (RGDP), GDP price index inflation (PGDP), real consumption (RCONSUM), Industrial production (INDPROD), real nonresidential investment (RNRESIN), real residential investment (RRESINV), real federal government consumption (RGF), real state and local government consumption (RGSL). Forecast of h period ahead: $F_{i,t}y_{t+h} = (\frac{F_{i,t}\widetilde{y}_{t+h}}{\widetilde{y}_{t+h-4}} - 1) \times 100$, where $F_{i,t}\widetilde{y}_{t+h}$ is the original survey forecast from the forecaster i provided in period t regarding the state variable $\widetilde{y}$ in h period ahead. $\widetilde{y}_{t+h-4}$ is the actual state value of period $t+h-4$ already released. The procedures are a replication of Bordalo et al. (2020).

Variables that are taken directly from the survey data include unemployment rate

(UNEMP), housing start (HOUSING), CPI, Three-month Treasury rate (Tbills), Ten-year Treasury rate (Tbonds).

A.2 Three years ahead forecast and forecasts of longer horizon

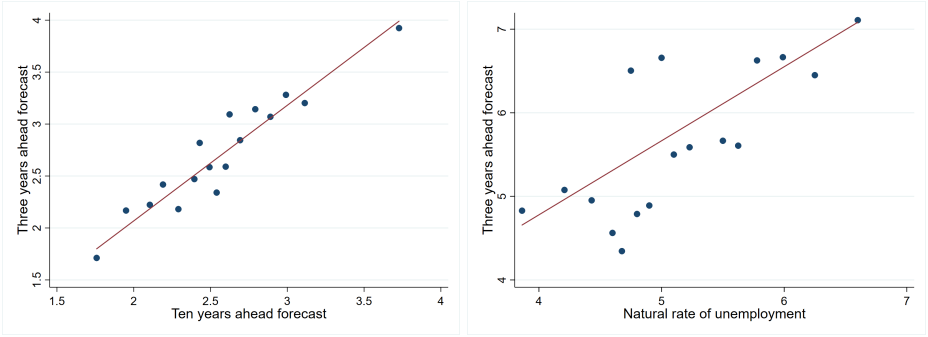

(a) Real GDP (b) Unemployment

Figure 8. *Three-year-ahead forecasts and forecasts for longer horizons. Note: The sample period is from 2009 to 2019, based on data availability. Forecasts of the natural unemployment rate are only available in the third quarter survey, while forecasts of ten-year-ahead real GDP are only available in the first quarter survey. Figure 8(a) illustrates the real GDP forecasts for three years ahead and ten years ahead. Figure 8(b) shows unemployment forecasts for three years ahead and the natural rate of unemployment. The correlation between the three-year horizon forecasts and longer-horizon forecasts, as depicted in the upper two figures, is 0.903 for real GDP growth and 0.886 for unemployment.*

A.3 Estimation Results: Covariance between changes in long-term forecasts and cyclical forecasts

Table 4. *Covariance between changes in long term forecasts and cyclical forecasts*

Covariance between changes in long term forecasts and cyclical forecasts			
	COV_F^h	95% bootstrap CI	Obs
Panel A. Unemployment rate			
$h = 0$	-0.203	(-0.244, -0.161)	794
$h = 1$	-0.192	(-0.232, -0.152)	815
$h = 2$	-0.177	(-0.214, -0.139)	819
$h = 3$	-0.164	(-0.199, -0.129)	817
$h = 4$	-0.151	(-0.183, -0.118)	818
Panel B. Real GDP growth			
$h = 0$	-0.219	(-0.273, -0.164)	783
$h = 1$	-0.214	(-0.271, -0.156)	781
$h = 2$	-0.204	(-0.260, -0.147)	785
$h = 3$	-0.204	(-0.258, -0.149)	785
$h = 4$	-0.202	(-0.256, -0.148)	785

Note: This table shows the covariance between the changes in long-term forecasts and cyclical forecasts. The sample period is from 2009Q2 to 2019Q4. Panel A shows the results of the unemployment rate, while Panel B shows the results of the Real GDP growth.

A.4 Robustness: ECB-SPF

This subsection presents estimation results using the European Central Bank's Survey of Professional Forecasters (ECB-SPF). The ECB-SPF is a quarterly survey collecting

data on expected inflation, real GDP growth, and unemployment rates in the euro area. Each quarter, approximately 50 professional forecasters participate, providing forecasts for the current and following year. Forecasts for two years ahead were available only in Q3 and Q4 surveys from 2001 to 2012, but have been included in all survey waves since 2013. Since 2001, the survey has included a question on long-term economic conditions. This question solicits forecasts for four years ahead in Q1 and Q2 surveys, and five years ahead in Q3 and Q4 surveys. We use these four- and five-year-ahead forecasts as our long-run forecasts.

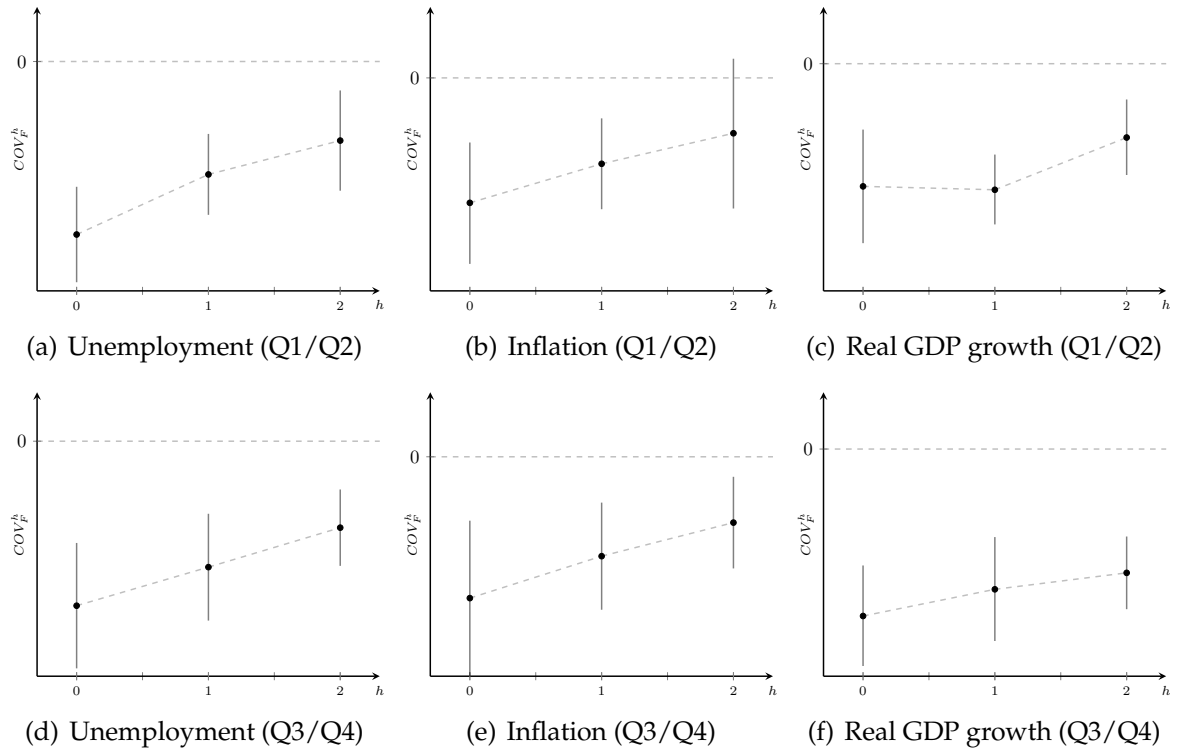

(a) Unemployment (Q1/Q2) (b) Inflation (Q1/Q2) (c) Real GDP growth (Q1/Q2)

(d) Unemployment (Q3/Q4) (e) Inflation (Q3/Q4) (f) Real GDP growth (Q3/Q4)

Figure 9. *Covariance between the changes in long-run forecasts and cyclical forecasts across forecast horizons h. Note: This figure illustrates the covariance COV_F^h for the unemployment rate, inflation and the real GDP growth across various forecast horizons h using the ECB-SPF data. The upper three figures show the estimation result using the Q1 and Q2 data. The lower three figures show the estimation result using the Q3 and Q4 data. In all cases, the covariance is negative and statistically significant, increasing as the forecast horizon extends. The black dots represent the estimates, and the gray solid lines denote the 95% confidence intervals. The sample period is from 2001Q1 to 2019Q4.*

Figure 9 presents the estimation results of Equation (1) using ECB-SPF data. Horizons $h = 0, 1, 2$ correspond to forecasts for the current year, one year ahead, and two years ahead, respectively. Because Q1/Q2 surveys request forecasts four years ahead, while Q3/Q4 surveys request forecasts five years ahead, we split the data into two subsamples. The upper panels of Figure 9 use the Q1/Q2 subsample (cyclical belief = h-horizon forecast minus four-year-ahead forecast). The lower panels use the Q3/Q4 subsample (cyclical belief = h-horizon forecast minus five-year-ahead forecast). For all

variables, the estimated coefficients COV_F^0 are negative, statistically significant, and increasing in h, consistent with the results in the main text.

Table 5 presents the estimation results from Equation (2) using ECB-SPF data. These results are consistent with those in the main text. For unemployment and real GDP growth, the estimated coefficients are statistically positive. For inflation, the coefficient is statistically positive but small when using forecast variance as the dispersion measure, and non-significant when using the interquartile range (75th minus 25th percentile).

Table 5. *Forecast dispersion over forecast horizon*

	Dependent Variable: Forecast Dispersion				
	Variance of forecasts		50 percentile difference		
	β_1	SE	β_1	SE	Obs
Forecast Variable	(1)	(2)	(3)	(4)	
Unemployment rate	0.122***	0.006	0.182***	0.007	280
Real GDP growth	0.006***	0.002	0.022***	0.005	280
Inflation rate	0.003**	0.001	0.002	0.004	280

Note: This table shows results from estimating Equation (2) using the ECB-SPF data. The sample period is from 2001Q1 to 2019Q4. In column (1), the dependent variable is the variance of forecasts across forecasters. In column (3), we use the difference between the 25% percentile and 50% percentile. Standard errors are clustered at the year-quarter level.

A.5 Robustness: Forecast dispersion over forecast horizon with time fixed effect

Table 6. *Forecast dispersion over forecast horizon with time FE*

	Dependent Variable: Forecast Dispersion					
	Variance of forecasts		50 percentile difference			
	β_1	SE	β_1	SE	Time FE	Obs
Forecast Variable	(1)	(2)	(3)	(4)		
Nominal GDP	0.337***	0.014	0.204***	0.005	Yes	1,025
Real GDP	0.242***	0.013	0.162***	0.004	Yes	1,025
GDP price index inflation	0.118***	0.005	0.119***	0.003	Yes	1,025
Real consumption	0.125***	0.008	0.127***	0.004	Yes	770
Industrial production	0.860***	0.034	0.320***	0.009	Yes	1,025
Real nonresidential investment	1.647***	0.068	0.497***	0.012	Yes	770
Real residential investment	6.021***	0.299	0.932***	0.026	Yes	770
Real federal government consumption	1.284***	0.065	0.393***	0.013	Yes	770
Real state and local government consumption	0.317***	0.016	0.210***	0.006	Yes	770
Housing start	0.004***	0.000	0.020***	0.001	Yes	1,024
Unemployment	0.034***	0.001	0.082***	0.002	Yes	1,014
Inflation rate (CPI)	-0.066***	0.013	-0.073***	0.008	Yes	770
Three-month Treasury rate	0.053***	0.002	0.106***	(0.003	Yes	770
Ten-year Treasury rate	0.045***	0.001	0.094***	0.002	Yes	560

Note: This table shows the coefficients from estimating Equation (2) with year-quarter fixed effect. The sample period is from 1968Q4 to 2019Q4. In column (1), the dependent variable is the variance of forecasts. In column (3), the dependent variable is the difference between the 25% percentile and 50% percentile. Standard errors are clustered at the year-quarter level.

A.6 Estimation procedures: Inflation

To estimate the set of parameters $\Theta = \{\rho, \sigma_\mu^2, \sigma_x^2, \sigma_e^2, \sigma_\epsilon^2\}$ before and after 2012, we begin by dividing the entire dataset into two subsets: one before 2012 and one after 2012. For each subset, we compute the average forecast variance for different forecast horizons ($h = 0, 1, 2, 3, 4$). These sets of forecast variances serve as the targets for estimation denoted as $\hat{m}$.

Since we want to capture the forecast variance across all the horizons, we give equal weights to all the targeted moments. Table 7 provides the summary statistic of the estimation moments.

Table 7. *Estimation Moments*

	Estimation Moments			
	Pre-2012		Post-2012	
	Target	SE	Target	SE
h=0	0.833	1.276	0.737	0.693
h=1	0.562	0.568	0.350	0.182
h=2	0.464	0.370	0.303	0.123
h=3	0.429	0.324	0.284	0.103
h=4	0.430	0.282	0.301	0.071

The distance is defined in Equation (16) as the weighted squared difference between the target moments $\hat{m}$ and the model prediction $m(\Theta)$, which represents the moments implied by the model for the given parameter set (Θ). Using MCMC with the Metropolis-Hastings algorithm, we choose the set of model parameters that minimize the distance $\Lambda(\Theta)$. The estimation of the parameter set before and after 2012 follows the exact same procedures, with different estimation targets derived from the respective subsets of the data.

B Proofs and Supplemental Material

B.1 Proofs

Proof of Lemma 1. To begin, we assume that the error term in the last period ($z_{i,t-1}$) is normally distributed with the variance $\sigma_{z,t-1}^2$. With the prior belief and the signal structures given by Equation (6) and (7), the posterior belief of forecaster i after receiv-

ing signals is given by:

$$
\begin{aligned}
p(\boldsymbol{\theta}|\boldsymbol{s}_{i,t}) &\propto p(\boldsymbol{\theta}^i_{2,t-1})p(\boldsymbol{s}_{i,t}|\boldsymbol{\theta}^i_{2,t-1}) \\
&\propto \exp\left\{-\frac{1}{2}[\boldsymbol{\theta}^T(\boldsymbol{\Sigma}_{\boldsymbol{s}}^{-1}+\boldsymbol{\Sigma}^{-1}_{\boldsymbol{\theta}^i_{2,t-1}})\boldsymbol{\theta}-2(\boldsymbol{\Sigma}_{\boldsymbol{s}}^{-1}+\boldsymbol{\Sigma}^{-1}_{\boldsymbol{\theta}^i_{2,t-1}})^{-1}(\boldsymbol{\Sigma}_{\boldsymbol{s}}^{-1}+\boldsymbol{\Sigma}^{-1}_{\boldsymbol{\theta}^i_{2,t-1}})(\boldsymbol{s}^T_{i,t}\boldsymbol{\Sigma}_{\boldsymbol{s}}^{-1}+\boldsymbol{\theta}^{i,T}_{2,t-1}\boldsymbol{\Sigma}^{-1}_{\boldsymbol{\theta}^i_{2,t-1}})\boldsymbol{\theta}]\right\} \\
&\propto \exp[-\frac{1}{2}(\boldsymbol{\theta}-\boldsymbol{\theta}^i_{1,t})^T(\boldsymbol{\Sigma}_{\boldsymbol{s}}^{-1}+\boldsymbol{\Sigma}^{-1}_{\boldsymbol{\theta}^i_{2,t-1}})(\boldsymbol{\theta}-\boldsymbol{\theta}^i_{1,t})],
\end{aligned}
$$

where

$$
\boldsymbol{\theta}^i_{1,t} = (\boldsymbol{\Sigma}_{\boldsymbol{s}}^{-1}+\boldsymbol{\Sigma}^{-1}_{\boldsymbol{\theta}^i_{2,t-1}})^{-1}(\boldsymbol{s}^T_{i,t}\boldsymbol{\Sigma}_{\boldsymbol{s}}^{-1}+\boldsymbol{\theta}^{i,T}_{2,t-1}\boldsymbol{\Sigma}^{-1}_{\boldsymbol{\theta}^i_{2,t-1}})^T.
$$

Therefore, $\mu^i_{1,t}$ and $x^i_{1,t}$ are joint normally distributed. To be specific, $\boldsymbol{\theta}^i_{1,t} = (\mu^i_{1,t}, x^i_{1,t})'$ is given by:

$$
\mu^i_{1,t} = \underbrace{\frac{\sigma^2_\epsilon(\rho^2\sigma^2_{z,t-1}+\sigma^2_x+\sigma^2_e)}{\Omega_t}}_{prior\ weight}\mu^i_{2,t-1} + \underbrace{\frac{V_t+\sigma^2_e(\sigma^2_{z,t-1}+\sigma^2_\mu)}{\Omega_t}}_{signal\ weight}s^\mu_{i,t} - \frac{\rho\sigma^2_\epsilon\sigma^2_{z,t-1}}{\Omega_t}\underbrace{(s^x_{i,t}-\rho x^i_{2,t-1})}_{surprise\ from\ cycle}, \tag{B1}
$$

$$
x^i_{1,t} = \underbrace{\frac{\sigma^2_e(\sigma^2_{z,t-1}+\sigma^2_\mu+\sigma^2_\epsilon)}{\Omega_t}}_{prior\ weight}\rho x^i_{2,t-1} + \underbrace{\frac{V_t+\sigma^2_\epsilon(\sigma^2_x+\rho^2\sigma^2_{z,t-1})}{\Omega_t}}_{signal\ weight}s^x_{i,t} - \frac{\rho\sigma^2_e\sigma^2_{z,t-1}}{\Omega_t}\underbrace{(s^\mu_{i,t}-\mu^i_{2,t-1})}_{surprise\ from\ trend}. \tag{B2}
$$

where Ω_t and V_t are constants:

$$
\Omega_t = (\sigma^2_{z,t-1}+\sigma^2_\mu+\sigma^2_\epsilon)(\sigma^2_x+\sigma^2_e+\rho^2\sigma^2_{z,t-1})-\rho^2\sigma^4_{z,t-1},\ V_t = (\sigma^2_{z,t-1}+\sigma^2_\mu)(\sigma^2_x+\rho^2\sigma^2_{z,t-1})-\rho^2\sigma^4_{z,t-1}.
$$

And the variance-covariance matrix of $\mu^i_{1,t}$ and $x^i_{1,t}$ is:

$$
(\boldsymbol{\Sigma}_{\boldsymbol{s}}^{-1}+\boldsymbol{\Sigma}^{-\mathbf{1}}_{\boldsymbol{\theta}^i_{2,t-1}})^{-1} = \begin{pmatrix} \mathrm{Var}^T_t & \widetilde{\mathrm{COV}}_t \\ \widetilde{\mathrm{COV}}_t & \mathrm{Var}^C_t \end{pmatrix} = \begin{pmatrix} \frac{\sigma^2_\epsilon[\Omega_t-\sigma^2_\epsilon(\sigma^2_x+\sigma^2_e+\rho^2\sigma^2_{z,t-1})]}{\Omega_t} & -\frac{\rho\sigma^2_e\sigma^2_\epsilon\sigma^2_{z,t-1}}{\Omega_t} \\ -\frac{\rho\sigma^2_e\sigma^2_\epsilon\sigma^2_{z,t-1}}{\Omega_t} & \frac{\sigma^2_e[\Omega_t-\sigma^2_\epsilon(\sigma^2_\epsilon+\sigma^2_\mu+\sigma^2_{z,t-1})]}{\Omega_t} \end{pmatrix}, \tag{B3}
$$

The observation of y_t provides new information and forecasters would update their beliefs accordingly:

$$f^i(\mu_t|y_t) \propto \exp\left\{-\frac{1}{2(1-r_t^2)}[\frac{(\mu_t-\mu_{1,t}^i)^2}{\text{Var}_t^T} - \frac{2r_t(\mu_t-\mu_{1,t}^i)(y_t-\mu_t-x_{1,t}^i)}{\sqrt{\text{Var}_t^T\text{Var}_t^C}} + \frac{(y_t-\mu_t-x_{1,t}^i)^2}{\text{Var}_t^C}]\right\}$$

$$\propto \exp\{-\frac{1}{2(1-r_t^2)}[\frac{(\text{Var}_t^T + 2r_t\sqrt{\text{Var}_t^T\text{Var}_t^C} + \text{Var}_t^C)\mu_t^2}{\text{Var}_t^T\text{Var}_t^C}$$

$$- 2\mu_t\frac{\text{Var}_t^C\mu_{1,t}^i + r_t\sqrt{\text{Var}_t^T\text{Var}_t^C}(\mu_{1,t}^i + y_t - x_{1,t}^i) + \text{Var}_t^T(y_t - x_{1,t}^i)}{\text{Var}_t^T\text{Var}_t^C}]\}, \tag{B4}$$

and

$$f^i(x_t|y_t) \propto \exp\left\{-\frac{1}{2(1-r_t^2)}[\frac{(y_t-x_t-\mu_{1,t}^i)^2}{\text{Var}_t^T} - \frac{2r_t(y_t-x_t-\mu_{1,t}^i)(x_t-x_{1,t}^i)}{\sqrt{\text{Var}_t^T\text{Var}_t^C}} + \frac{(x_t-x_{1,t}^i)^2}{\text{Var}_t^C}]\right\}$$

$$\propto \exp\{-\frac{1}{2(1-r_t^2)}(\frac{\text{Var}_t^T + 2r_t\sqrt{\text{Var}_t^T\text{Var}_t^C} + \text{Var}_t^T)x_t^2}{\text{Var}_t^T\text{Var}_t^C})$$

$$- 2x_t\frac{\text{Var}_t^C(y_t - \mu_{1,t}^i) + r_t\sqrt{\text{Var}_t^T\text{Var}_t^C}(y_t - \mu_{1,t}^i + x_{1,t}^i) + \text{Var}_t^T x_{1,t}^i}{\text{Var}_t^T\text{Var}_t^C}\}, \tag{B5}$$

where r_t is given by:

$$r_t = \frac{\widetilde{\text{COV}}_t}{\sqrt{\text{Var}_t^T\text{Var}_t^C}}. \tag{B6}$$

According to Equations (B4) and (B5), the posterior beliefs $f^i(\mu_t|y_t)$ and $f^i(x_t|y_t)$ are normal distributions. Therefore, $\mu_{2,t}^i$ and $x_{2,t}^i$ are normally distributed. As a result, $z_{i,t}$ will also be normally distributed. That shows first part of the lemma.

Furthermore, the means of the posterior beliefs are given by:

$$\mu_{2,t}^i = \frac{\text{Var}_t^C\mu_{1,t}^i + \text{Var}_t^T(y_t - x_{1,t}^i) + r_t\sqrt{\text{Var}_t^T\text{Var}_t^C}(\mu_{1,t}^i + y_t - x_{1,t}^i)}{\text{Var}_t^T + 2r_t\sqrt{\text{Var}_t^T\text{Var}_t^C} + \text{Var}_t^C}$$

$$= \frac{(\text{Var}_t^C + \widetilde{\text{COV}}_t)\mu_{1,t}^i + (\text{Var}_t^T + \widetilde{\text{COV}}_t)(y_t - x_{1,t}^i)}{\text{Var}_t^T + \text{Var}_t^C + 2\widetilde{\text{COV}}_t}. \tag{B7}$$

and

$$x_{2,t}^i = \frac{\text{Var}_t^C(y_t - \mu_{1,t}^i) + r_t\sqrt{\text{Var}_t^T\text{Var}_t^C}(y_t - \mu_{1,t}^i + x_{1,t}^i) + \text{Var}_t^T x_{1,t}^i}{\text{Var}_t^T + 2r_t\sqrt{\text{Var}_t^T\text{Var}_t^C} + \text{Var}_t^C}$$

$$= \frac{(\text{Var}_t^C + \widetilde{\text{COV}}_t)(y_t - \mu_{1,t}^i) + (\text{Var}_t^T + \widetilde{\text{COV}}_t)x_{1,t}^i}{\text{Var}_t^T + \text{Var}_t^C + 2\widetilde{\text{COV}}_t}.$$

We show that

$$\begin{aligned}\mu^i_{2,t} + x^i_{2,t} &= \frac{(\mathrm{Var}^C_t + \widetilde{\mathrm{COV}}_t)\mu^i_{1,t} + (\mathrm{Var}^T_t + \widetilde{\mathrm{COV}}_t)(y_t - x^i_{1,t})}{\mathrm{Var}^T_t + \mathrm{Var}^C_t + 2\widetilde{\mathrm{COV}}_t} \\ &+ \frac{(\mathrm{Var}^C_t + \widetilde{\mathrm{COV}}_t)(y_t - \mu^i_{1,t}) + (\mathrm{Var}^T_t + \widetilde{\mathrm{COV}}_t)x^i_{1,t}}{\mathrm{Var}^T_t + \mathrm{Var}^C_t + 2\widetilde{\mathrm{COV}}_t} \\ &= y_t.\end{aligned}$$

The second part of the lemma is shown.

Proof of Lemma 2. We first establish the existence of the steady state and then show that the steady state is unique. According to Equations (B4) and (B5), after observing y_t, the variance of the separation error is given by:

$$\sigma^2_{z_t} = \frac{(1 - r_t^2)\mathrm{Var}^T_t \mathrm{Var}^C_t}{\mathrm{Var}^T_t + 2r_t\sqrt{\mathrm{Var}^T_t \mathrm{Var}^C_t} + \mathrm{Var}^C_t}. \tag{B8}$$

Recall the definitions of Var^T_t, Var^C_t and r_t in Equations (B3) and (B6), we notice that the right-hand-side of Equation (B8) is a function of $\sigma^2_{z,t-1}$. Therefore, the steady state value σ^2_z is a fixed point of the condition characterized by Equation (B8). Solving for the fixed point of Equation (B8) gives:

$$\sigma^2_z = \frac{-\sigma^2_\mu[\Lambda + 2\rho(1-\rho)\sigma^2_e\sigma^2_\epsilon] + \sqrt{\sigma^2_\mu\Lambda[\sigma^2_\mu(\Lambda + 4\rho\sigma^2_e\sigma^2_\epsilon) + 4\sigma^2_e\sigma^2_\epsilon\sigma^2_x]}}{2[\Lambda + \rho^2\sigma^2_\mu(\sigma^2_e + \sigma^2_\epsilon)]}, \tag{B9}$$

where $\Lambda = (1-\rho)^2\sigma^2_e\sigma^2_\epsilon + \sigma^2_x(\sigma^2_e + \sigma^2_\epsilon)$.

In the next step, we demonstrate that regardless of the initial variance of the separation error, denoted as $\sigma^2_{z_0}$, it always converges to a unique steady state value σ^2_z. We first simplify Equation (B8) to:

$$\sigma^2_{z,t} = \frac{g_1(\sigma^2_{z,t-1})}{g_2(\sigma^2_{z,t-1})}, \tag{B10}$$

where

$$g_1(\sigma^2_{z,t-1}) = w_1\sigma^2_{z,t-1} + \eta_1 \quad \text{and} \quad g_2(\sigma^2_{z,t-1}) = w_2\sigma^2_{z,t-1} + \eta_2,$$

$$w_1 = \sigma^2_e\sigma^2_\epsilon(\rho^2\sigma^2_\mu + \sigma^2_x);\ \eta_1 = \sigma^2_e\sigma^2_\epsilon\sigma^2_\mu\sigma^2_x;$$

$$w_2 = \rho^2(\sigma^2_e\sigma^2_\epsilon + \sigma^2_e\sigma^2_\mu + \sigma^2_\mu\sigma^2_\epsilon) + \sigma^2_e\sigma^2_\epsilon + \sigma^2_e\sigma^2_x + \sigma^2_\epsilon\sigma^2_x - 2\rho\sigma^2_e\sigma^2_\epsilon;\ \eta_2 = \sigma^2_e\sigma^2_\epsilon(\sigma^2_\mu + \sigma^2_x) + \sigma^2_\mu\sigma^2_x(\sigma^2_e + \sigma^2_\epsilon).$$

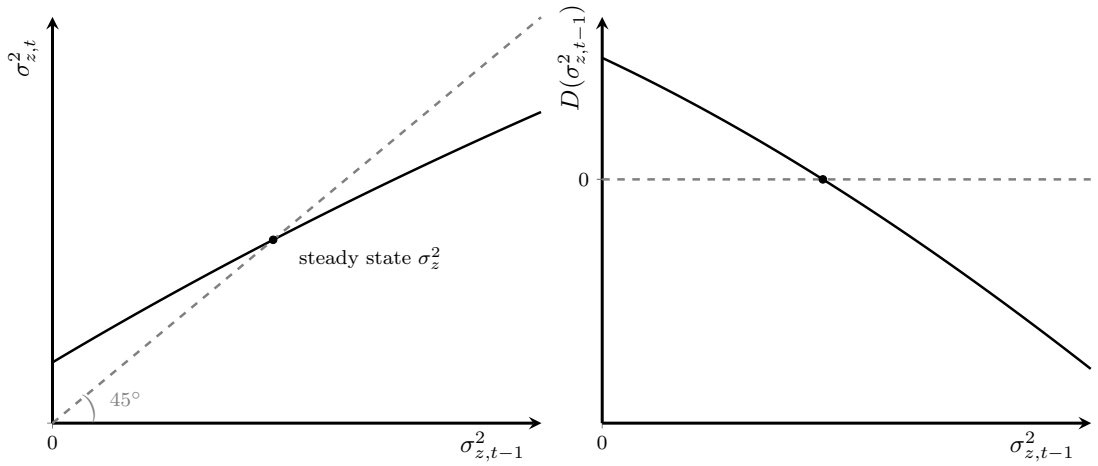

(a) $\sigma^2_{z,t-1}$ and $\sigma^2_{z,t}$ (b) $D(\sigma^2_{z,t-1})$ and $\sigma^2_{z,t-1}$

Figure 10. *The relationship between $\sigma^2_{z,t-1}$ and $\sigma^2_{z,t}$.*

Define the difference between $\sigma^2_{z,t}$ and $\sigma^2_{z,t-1}$ as:

$$D(\sigma^2_{z,t-1}) = \sigma^2_{z,t} - \sigma^2_{z,t-1} = \frac{g_1(\sigma^2_{z,t-1})}{g_2(\sigma^2_{z,t-1})} - \sigma^2_{z,t-1}.$$

To show the steady state is unique, it is sufficient to show that $D(\sigma^2_{z,t-1})$ is monotonically decreasing. We first show that evaluated at $\sigma^2_{z,t-1} = 0$, the derivative is negative.

$$\frac{\partial D(\sigma^2_{z,t-1})}{\partial \sigma^2_{z,t-1}}|_{\sigma^2_{z,t-1}=0} = \left[\frac{\sigma^2_e\sigma^2_\epsilon(\rho\sigma^2_\mu + \sigma^2_x)}{\sigma^2_e\sigma^2_\epsilon(\rho\sigma^2_\mu + \sigma^2_x) + \sigma^2_\mu\sigma^2_x(\sigma^2_e + \sigma^2_\epsilon)}\right]^2 - 1 < 0.$$

Then we show that the first-order derivative of $D(\sigma^2_{z,t-1})$ is negative. The derivative is given by:

$$\frac{\partial D(\sigma^2_{z,t-1})}{\partial \sigma^2_{z,t-1}} = \frac{w_1\eta_2 - w_2\eta_1}{(w_2\sigma^2_{z,t} + \eta_2)^2} - 1 = \left[\frac{\sigma^2_e\sigma^2_\epsilon(\rho\sigma^2_\mu + \sigma^2_x)}{(w_2\sigma^2_{z,t} + \eta_2)}\right]^2 - 1. \tag{B11}$$

It is always decreasing, because we show that the second-order derivative is negative:

$$\frac{\partial^2 D(\sigma^2_{z,t-1})}{\partial(\sigma^2_{z,t-1})^2} = -2w_2\frac{[\sigma^2_e\sigma^2_\epsilon(\rho\sigma^2_\mu + \sigma^2_x)]^2}{(w_2\sigma^2_{z,t} + \eta_2)^3} < 0.$$

Since $D(\sigma^2_{z,t})$ is monotonously decreasing and concave and the steady state exists, it is unique. Figure 10(a) illustrates the relationship between $\sigma^2_{z,t-1}$ and $\sigma^2_{z,t}$, while Figure 10(b) further illustrates how the difference between the two variances (i.e., $\sigma^2_{z,t} - \sigma^2_{z,t-1}$) responds to $\sigma^2_{z,t-1}$, highlighting the convergence property.

Proof of Lemma 3. Given the quadratic utility function, the forecaster's optimal forecasts are given by the following:

$$\begin{aligned} F_{i,t}y_{t+h} &= E_{i,t}[y_{t+h}] \\ &= E_{i,t}[\mu_t + \rho^h x_t] \\ &= \mu^i_{1,t} + \rho^h x^i_{1,t}. \end{aligned}$$

The first equality is derived from the first order condition of the standard quadratic utility function. With a quadratic utility function, forecasters would minimize the expected squared error, and the first-order condition is given by:

$$E_{i,t}[F_{i,t}y_{t+h} - y_{t+h}] = 0.$$

The second equality follows given the data generation process is known to forecasters. The third equality states that the expected value of the sum of μ_t and $\rho^h x_t$ is the sum of the expected values of the two components, a well known property using Fourier transform (Folland 2009).

Proof of Lemma 4. From Equation (B7) in the proof of Lemma 2, we obtain:

$$\begin{aligned} z_{i,t-1} &= \mu^i_{2,t-1} - \mu_{t-1} \\ &= \frac{(\mathrm{Var}^T + \widetilde{\mathrm{COV}})(x_{t-1} - x^i_{1,t-1}) - (\mathrm{Var}^C + \widetilde{\mathrm{COV}})(\mu_{t-1} - \mu^i_{1,t-1})}{\mathrm{Var}^T + \widetilde{\mathrm{COV}} + \mathrm{Var}^C + \widetilde{\mathrm{COV}}}, \end{aligned}$$

which is the first part of Lemma 4.

For the second part of Lemma 4, we show the steady state value of σ^2_z increases in σ^2_μ. Our idea is to show that the solid line in Figure 10(a) shifts upwards when σ^2_μ is larger. Towards this end, we prove the following claim.

Claim 1. For any given $\sigma^2_{z,t-1}$, the induced $\sigma^2_{z,t}$ is increasing in σ^2_μ.

Using Equation (B10), we obtain the derivative:

$$\frac{\partial \sigma^2_{z,t}}{\partial \sigma^2_\mu} = \frac{\partial [g_1(\sigma^2_{z,t-1})/g_2(\sigma^2_{z,t-1})]}{\partial \sigma^2_\mu} = \frac{\sigma^4_e \sigma^4_\epsilon [\sigma^2_x - \rho(1-\rho)\sigma^2_{z,t-1}]^2}{g_2(\sigma^2_{z,t-1})^2} > 0. \tag{B12}$$

The claim is shown. Consequently, given the properties of $D(\sigma^2_{z,t-1})$ shown earlier, a larger steady state value for σ^2_z is implied. The comparative statics with respect to σ^2_x, σ^2_ϵ, and σ^2_e are analogous.

It is worth noting that $z_{i,t}$ is obtained via Bayesian updating, using the prior belief

$\mu^i_{1,t}$ and $y_t - x^i_{1,t}$ shown in Equation (B9). As the variance of the posterior belief is always smaller than the variance of both prior beliefs, we can obtain:

$$0 \leq \sigma_z^2 \leq \min\{\text{Var}^C, \text{Var}^T\}.$$

In a special case when the variance of private signals go to infinity (i.e., $\sigma_e^2 \to +\infty$, $\sigma_\epsilon^2 \to +\infty$), the steady state σ_z^2 is:

$$\sigma_z^2 = \frac{-(1-\rho^2)\sigma_\mu^2 + \sqrt{\sigma_\mu^2(1-\rho)^2[(1+\rho)^2\sigma_\mu^2 + 4\sigma_x^2]}}{2(1-\rho)^2}$$

Similarly, considering the case that when the persistence of the cyclical component ρ changes:

$$\frac{\partial \sigma_{z,t}^2}{\partial \rho} = \frac{\sigma_{z,t-1}^2}{g_2(\sigma_{z,t-1}^2)^2}\left\{2\sigma_e^4\sigma_\epsilon^4[\rho\sigma_\mu^2 + \sigma_x^2][\sigma_\mu^2 + (1-\rho)\sigma_{z,t-1}^2]\right\} > 0.$$

Therefore, the steady state value of σ_z^2 is increasing in ρ. The logic underlying this statement is analogous.

Proof of Proposition 1. To show the first item, we note the following. When $\sigma_\mu^2 = 0$, according to Lemma 4, σ_z^2 goes to zero, and therefore $\widetilde{\text{COV}}$ becomes zero. When $\sigma_\mu^2 \to +\infty$, Lemma 4 states that $\sigma_z^2 \to \min\{\text{Var}^C, \text{Var}^T\}$, but $\Omega \to +\infty$ in this case. Therefore, $\widetilde{\text{COV}}$ goes to zero.

To show the second term, we first show that the second order derivative of σ_z^2 with respect to σ_μ^2 is negative. In Equation (B12), $g_2(\sigma_{z,t-1}^2)^2$ increases in σ_μ^2. Then the derivative $\partial\sigma_z^2/\partial\sigma_\mu^2$ decreases when σ_μ^2 is larger. As σ_μ^2 approaches infinity, $\partial\sigma_z^2/\partial\sigma_\mu^2$ approaches zero. That is,

$$Z'_\mu \equiv \frac{\partial \sigma_z^2}{\partial \sigma_\mu^2} > 0 \quad \text{and} \quad Z''_\mu \equiv \frac{\partial^2 \sigma_z^2}{(\partial \sigma_\mu^2)^2} < 0.$$

We then derive the derivative with respect to σ_μ^2:

$$\frac{\partial|\widetilde{\text{COV}}|}{\partial \sigma_\mu^2} \propto Z'_\mu(\sigma_e^2 + \sigma_x^2)(\sigma_\epsilon^2 + \sigma_\mu^2) - \sigma_z^2(\rho^2\sigma_z^2 + \sigma_e^2 + \sigma_x^2).$$

We show that evaluated at $\sigma_\mu^2 = 0$,

$$\frac{\partial|\widetilde{\text{COV}}|}{\partial \sigma_\mu^2}|_{\sigma_\mu^2=0} \propto Z'_\mu(\sigma_e^2 + \sigma_x^2)\sigma_\epsilon^2 > 0.$$

That is because $\sigma_z^2 = 0$ when $\sigma_\mu^2 = 0$. The second-order derivative is given by:

$$\frac{\partial^2 |\widetilde{\text{COV}}|}{(\partial \sigma_\mu^2)^2} \propto Z''_\mu(\sigma_\mu^2 + \sigma_\epsilon^2)(\sigma_e^2 + \sigma_x^2) - 2\rho^2\sigma_z^2 Z'_\mu < 0.$$

To see the inequality we note that $Z'_\mu > 0$, and $Z''_\mu < 0$. Therefore, there exists a unique $\widetilde{\sigma}_\mu^2 > 0$, such that $\partial|\widetilde{\text{COV}}|/\partial\sigma_\mu^2 = 0$. For any $\sigma_\mu^2 < \widetilde{\sigma}_\mu^2$, $|\widetilde{\text{COV}}|$ is increasing in σ_μ^2; and for any $\sigma_\mu^2 > \widetilde{\sigma}_\mu^2$, $|\widetilde{\text{COV}}|$ is decreasing in σ_μ^2. The property that $|\widetilde{\text{COV}}|$ increases and then decrease is implied.

It is straightforward to show the second item that $|\widetilde{\text{COV}}|$ is always increasing in ρ, because

$$\frac{\partial|\widetilde{\text{COV}}|}{\partial\rho} = \frac{\sigma_e^2\sigma_\epsilon^2}{\Omega^2}\left\{(\sigma_x^2 + \sigma_e^2)[\sigma_z^4 + \rho Z'_\rho(\sigma_\mu^2 + \sigma_\epsilon^2)] + \sigma_z^2(\sigma_\mu^2 + \sigma_\epsilon^2)[\sigma_x^2 + \sigma_e^2 - \rho^2\sigma_z^2]\right\} > 0,$$

where $Z'_\rho \equiv \partial\sigma_z^2/\partial\rho > 0$.

Proof of Proposition 2. The covariance between the changes in the long term forecasts and the cyclical forecasts is given by:

$$\begin{aligned} COV_F^h &= cov(F_{i,t}y_{t+3Y} - F_{i,t-1}y_{t-1+3Y}, Cyc_{i,t}^h - Cyc_{i,t-1}^h) \\ &= (\rho^h - \rho^{3Y})\left[cov(\mu_{1,t}^i - \mu_{1,t-1}^i, x_{1,t}^i - x_{1,t-1}^i) + \rho^{3Y} var(x_{1,t}^i - x_{1,t-1}^i)\right] \\ &= (\rho^h - \rho^{3Y})(\widetilde{\text{COV}} + \rho^{3Y}\text{Var}^C) \\ &= \frac{(\rho^h - \rho^{3Y})\sigma_e^2}{\Omega}\left\{\rho^{3Y}[\Omega - \sigma_e^2(\sigma_\epsilon^2 + \sigma_\mu^2 + \sigma_z^2)] - \rho\sigma_\epsilon^2\sigma_z^2\right\} \\ &\propto \rho^{3Y}[\Omega - \sigma_e^2(\sigma_\epsilon^2 + \sigma_\mu^2 + \sigma_z^2)] - \rho\sigma_\epsilon^2\sigma_z^2. \end{aligned} \tag{B13}$$

Define $K \equiv \rho^{3Y}[\Omega - \sigma_e^2(\sigma_\epsilon^2 + \sigma_\mu^2 + \sigma_z^2)] - \rho\sigma_\epsilon^2\sigma_z^2$. Then the sign of the covariance between changes in trend forecasts and changes in cyclical forecasts depends on the sign of K.

To prove the properties in the proposition, we first show that for any given σ_μ^2, there is a threshold $\overline{\sigma}_x^2$ such that if and only if $\sigma_x^2 < \overline{\sigma}_x^2$, then $K < 0$; and otherwise, $K \geq 0$. To see this, we derive the first-order derivative of K with respect to σ_x^2:

$$\begin{aligned} \frac{\partial K}{\partial\sigma_x^2} &= \rho^{3Y}[\sigma_z^2 + \sigma_\mu^2 + \sigma_\epsilon^2 + \sigma_x^2 Z'_x + \rho^2 Z'_x(\sigma_\mu^2 + \sigma_\epsilon^2)] - \rho\sigma_\epsilon^2 Z'_x \\ &= Z'_x\left[\rho^{3Y}\left(\frac{\sigma_z^2 + \sigma_\mu^2 + \sigma_\epsilon^2}{Z'_x} + \sigma_x^2 + \rho^2\sigma_\mu^2 + \rho^2\sigma_\epsilon^2\right) - \rho\sigma_\epsilon^2\right]. \end{aligned} \tag{B14}$$

According to Lemma 4, $Z'_x > 0$ and $Z''_x < 0$. Therefore, the sum of first two terms in

Equation (B14), $(\sigma_z^2 + \sigma_\mu^2 + \sigma_\epsilon^2)/Z'_x + \sigma_x^2$, increases in σ_x^2.

If $\partial K/\partial \sigma_x^2 \geq 0$ when evaluated at $\sigma_x^2 = 0$, then it always holds $\partial K/\partial \sigma_x^2 \geq 0$. If $\partial K/\partial \sigma_x^2 < 0$ when evaluated at $\sigma_x^2 = 0$, $\partial K/\partial \sigma_x^2$ crosses zero only once from below. Note that $\partial K/\partial \sigma_x^2$ must be positive when σ_x^2 is sufficiently large.

Furthermore, we characterize how K changes in σ_x^2. When $\sigma_x^2 = 0$, $K = 0$. That is because $\sigma_z^2 = 0$. When $\sigma_x^2 > 0$, K is either always positive, or K initially decreases and then crosses zero from below. This property implies that for any given value of σ_μ^2, there exists a threshold $\overline{\sigma}_x^2 \geq 0$, such that $K|_{\sigma_x^2 = \overline{\sigma}_x^2} = 0$, and for any $\sigma_x^2 < \overline{\sigma}_x^2$, $K < 0$.

Given this property, we start proving the first item in this proposition. Towards this end, we show the following claim.

Claim: When $\sigma_x^2 = 0$, there exists a threshold $\overline{\sigma}_\mu^2$ for σ_μ^2, such that when $\sigma_\mu^2 \geq \overline{\sigma}_\mu^2$, $\overline{\sigma}_x^2 = 0$; when $0 < \sigma_\mu^2 < \overline{\sigma}_\mu^2$, $\overline{\sigma}_x^2 > 0$; and when $\sigma_\mu^2 = 0$, $\overline{\sigma}_x^2 = 0$.

To prove this claim, we first evaluate $\partial K/\partial \sigma_x^2$ at $\sigma_x^2 = 0$:

$$\frac{\partial K}{\partial \sigma_x^2}|_{\sigma_x^2=0} = Z'_{x=0}\left[\rho^{3Y}\left(\frac{\sigma_\mu^2 + \sigma_\epsilon^2}{Z'_{x=0}} + \rho^2\sigma_\mu^2 + \rho^2\sigma_\epsilon^2\right) - \rho\sigma_\epsilon^2\right],$$

where $Z'_{x=0}$ is derivative of σ_z^2 evaluated at $\sigma_x^2 = 0$. It is given by:

$$Z'_{x=0} \equiv \frac{\partial \sigma_z^2}{\partial \sigma_x^2}|_{\sigma_x^2=0} = \begin{cases} \frac{2\rho(\sigma_e^2+\sigma_\epsilon^2)}{(1-\rho)(1+\rho)}\sigma_\mu^2 + \frac{2\sigma_e^2\sigma_\epsilon^2}{1+\rho}, & \text{if } \sigma_\mu^2 > 0. \\ 0, & \text{if } \sigma_\mu^2 = 0. \end{cases} \tag{B15}$$

There are only two cases. (i) When $\partial K/\partial \sigma_x^2|_{\sigma_x^2=0} \geq 0$, then K is always positive when $\sigma_x^2 > 0$ and $\overline{\sigma}_x^2 = 0$; and (ii) when $\partial K/\partial \sigma_x^2|_{\sigma_x^2=0} < 0$, K is negative and then crosses zero from below at $\sigma_x^2 = \overline{\sigma}_x^2 > 0$. Therefore, the necessary and sufficient condition for $\overline{\sigma}_x^2 > 0$ is given by $\partial K/\partial \sigma_x^2|_{\sigma_x^2=0} < 0$, which is equivalent to

$$\rho^{3Y}\left(\frac{\sigma_\mu^2 + \sigma_\epsilon^2}{Z'_{x=0}} + \rho^2\sigma_\mu^2 + \rho^2\sigma_\epsilon^2\right) - \rho\sigma_\epsilon^2 < 0$$

or using the expression of $Z'_{x=0}$ in Equation (B15),

$$\frac{2\rho^4(\sigma_e^2 + \sigma_\epsilon^2)}{1-\rho^2}(\sigma_\mu^2)^2 + \left[1 + \frac{2\rho^2\sigma_e^2\sigma_\epsilon^2}{1+\rho}(1 + \rho^2 - \rho^{1-3Y})\right]\sigma_\mu^2 - \left[\rho(\rho^{-h} - 1)\frac{2\sigma_e^2\sigma_\epsilon^2}{1+\rho} + \rho^{1-3Y}\right]\sigma_\epsilon^2 < 0. \tag{B16}$$

The left-hand-side of Equation (B16) is quadratic in σ_μ^2, therefore there are two roots. Note that The left-hand-side of Equation (B16) is decreasing and then increasing in σ_μ^2 and it is negative when $\sigma_\mu^2 = 0$. Therefore, there must exist a unique positive root

$\overline{\sigma}_\mu^2 > 0$.

Therefore, when $\sigma_\mu^2 \geq \overline{\sigma}_\mu^2$, $\overline{\sigma}_x^2 = 0$, which implies $K > 0$ on condition that $\sigma_x^2 > 0$. The first item in this proposition is shown. When $0 < \sigma_\mu^2 < \overline{\sigma}_\mu^2$, $\overline{\sigma}_x^2 > 0$, which implies $K > 0$ on condition that $\sigma_x^2 > \overline{\sigma}_x^2$. The second item is shown.

In addition, from the third equivalent of Equation (B13), as the forecast horizon h used to construct the cyclical forecast increases, the magnitude of COV_F^h is decreasing. The third item is shown.

Proof of Proposition 3. Given the optimal forecasts characterized by Lemma 3, the forecast variance across all forecasters is given by:

$$Var(F_{i,t}y_{t+h}) = E[(\mu_{1,t}^i - \overline{E}[\mu_t])^2] + \rho^{2h}E[(x_{1,t}^i - \overline{E}[x_t])^2] + 2\rho^h E[(\mu_{1,t}^i - \overline{E}[\mu_t])]E[(x_{1,t}^i - \overline{E}[x_t])].$$

$\overline{E}[\cdot]$ stands for the mean forecast across all forecasters. To be specific:

$$E[(\mu_{1,t}^i - \overline{E}[\mu_t])^2] = \text{Var}^T - \frac{\sigma_\epsilon^4(\rho^2\sigma_z^2 + \sigma_x^2 + \sigma_e^2)^2}{\Omega^2} - \frac{\rho^2\sigma_\epsilon^4\sigma_z^4}{\Omega^2} - \frac{\sigma_\epsilon^4(\sigma_e^2 + \sigma_x^2)^2}{\Omega^2} = \text{Var}^T\phi^T,$$

where ϕ^T is given by:

$$\begin{aligned}\phi^T &= 1 - \frac{\sigma_\epsilon^4}{\text{Var}^T} \times \frac{\sigma_\mu^2(\rho^2\sigma_z^2 + \sigma_x^2 + \sigma_e^2)^2 + \rho^2\sigma_x^2\sigma_z^4 + (\sigma_e^2 + \sigma_x^2)^2 W\sigma_z^2}{\Omega^2} \\ &= \frac{[V + \sigma_e^2(\sigma_\mu^2 + \sigma_z^2)]^2 + \rho^2\sigma_e^2\sigma_\epsilon^2\sigma_z^4 + \sigma_\epsilon^2(\sigma_e^2 + \sigma_x^2)^2 W\sigma_z^2}{\Omega[\Omega - \sigma_\epsilon^2(\sigma_x^2 + \sigma_e^2 + \rho^2\sigma_z^2)]} < 1.\end{aligned}$$

Note that $W = E[(z_{i,t-1} - \overline{E}[z_{i,t-1}])^2]/\sigma_z^2$ is a positive scalar in steady state and invariant in t. To obtain the numerator term $E[(z_{i,t} - \overline{E}[z_{i,t}])^2]$, we rewrite Equation (10) and express $z_{i,t}$ as the follows:

$$\begin{aligned}z_{i,t} = &\frac{\sigma_e^2\sigma_\epsilon^2}{\Omega(\text{Var}^T + 2\widetilde{\text{COV}} + \text{Var}^C)}\{-[\sigma_x^2 + \rho(\rho-1)\sigma_z^2]\gamma_t^\mu + [\sigma_\mu^2 + (1-\rho)\sigma_z^2]\gamma_t^x \\ &+ \sigma_e^2 V\epsilon_{i,t} - \sigma_\epsilon^2 Ve_{i,t} + (\rho\sigma_\mu^2 + \sigma_x^2)z_{i,t-1}\}.\end{aligned} \tag{B17}$$

This allows us to obtain:

$$z_{i,t} - \overline{E}[z_{i,t}] = \frac{\sigma_e^2\sigma_\epsilon^2}{\Omega(\text{Var}^T + 2\widetilde{\text{COV}} + \text{Var}^C)}\left[\sigma_e^2 V\epsilon_{i,t} - \sigma_\epsilon^2 Ve_{i,t} + (\rho\sigma_\mu^2 + \sigma_x^2)(z_{i,t-1} - \overline{E}[z_{i,t-1}])\right].$$

and

$$E[(z_{i,t} - \overline{E}[z_{i,t}])^2] = \frac{(\sigma_e^2 + \sigma_\epsilon^2)\sigma_z^2 V^2}{(\sigma_e^2 + \sigma_\epsilon^2)V^2 + \sigma_e^2\sigma_\epsilon^2\{\sigma_\mu^2[\sigma_x^2 + \rho\sigma_z^2(\rho-1)]^2 + \sigma_x^2[\sigma_\mu^2 + (1-\rho)\sigma_z^2]^2\}}.$$

Therefore, W is given by:

$$W = \frac{(\sigma_e^2 + \sigma_\epsilon^2)V^2}{(\sigma_e^2 + \sigma_\epsilon^2)V^2 + \sigma_e^2\sigma_\epsilon^2\{\sigma_\mu^2[\sigma_x^2 + \rho\sigma_z^2(\rho-1)]^2 + \sigma_x^2[\sigma_\mu^2 + (1-\rho)\sigma_z^2]^2\}} < 1.$$

Similarly, $E[(x_{1,t}^i - \overline{E}[x_t])^2]$ and $E[(\mu_{1,t}^i - \overline{E}[\mu_t])]E[(x_{1,t}^i - \overline{E}[x_t])]$ can be written as:

$$E[(x_{1,t}^i - \overline{E}[x_t])^2] = \frac{[V + \sigma_\epsilon^2(\sigma_x^2 + \rho^2\sigma_z^2)]^2 + \rho^2\sigma_e^2\sigma_\epsilon^2\sigma_z^4 + \rho^2\sigma_e^2(\sigma_\epsilon^2 + \sigma_\mu^2)^2 W\sigma_z^2}{\Omega[\Omega - \sigma_e^2(\sigma_\epsilon^2 + \sigma_\mu^2 + \sigma_z^2)]}\text{Var}^C = \phi^C\text{Var}^C,$$

and

$$\begin{aligned}
&E[(\mu_{1,t}^i - \overline{E}[\mu_t])]E[(x_{1,t}^i - \overline{E}[x_t])] \\
&= \frac{\sigma_\epsilon^2[V + \sigma_\epsilon^2(\sigma_x^2 + \rho^2\sigma_z^2)] + \sigma_e^2[V + \sigma_e^2(\sigma_z^2 + \sigma_\mu^2)] + \sigma_e^2\sigma_\epsilon^2(\sigma_x^2 + \sigma_e^2)(\sigma_\epsilon^2 + \sigma_\mu^2)W\sigma_z^2}{\Omega\sigma_e^2\sigma_\epsilon^2}\widetilde{\text{COV}} \\
&= \phi^{COV}\widetilde{\text{COV}}.
\end{aligned}$$

Therefore, the forecast variance of $F_{i,t}y_{t+h}$ across all forecasters can be written as:

$$Var(F_{i,t}y_{t+h}) = E[(F_{i,t}y_{t+h} - \overline{E}[F_{i,t}y_{t+h}])^2] = \rho^{2h}\text{Var}^C\phi^C + \text{Var}^T\phi^T + 2\rho^h\widetilde{\text{COV}}\phi^{COV},$$

Take the derivative with respect to the forecast horizon h:

$$\frac{\partial Var(F_{i,t}y_{t+h})}{\partial h} = 2\rho^h \ln\rho(\rho^h\text{Var}^C\phi^C + \widetilde{\text{COV}}\phi^{COV}).$$

The forecast variance is increasing in h if and only if $\partial Var(F_{i,t}y_{t+h})/\partial h > 0$. That is,

$$h > \underline{h} = \frac{1}{\ln\rho}\ln\frac{-\widetilde{\text{COV}}\phi^{COV}}{\text{Var}^C\phi^C}.$$

Proof of Proposition 4. Using Equation (8), the individual level beliefs can be rewritten as:

$$\boldsymbol{\theta}_{1,t}^i = (\boldsymbol{I} - \boldsymbol{\kappa})\boldsymbol{\theta}_{2,t-1}^i + \boldsymbol{\kappa}\boldsymbol{s}_{i,t},$$

and therefore, the consensus level belief is:

$$\boldsymbol{\theta}_{1,t} = (\boldsymbol{I} - \boldsymbol{\kappa})\boldsymbol{\theta}_{2,t-1} + \boldsymbol{\kappa}\boldsymbol{\theta}_t.$$

Therefore, the error term $\boldsymbol{\theta} - \boldsymbol{\theta}_{1,t}$ is:

$$\begin{aligned}\boldsymbol{\theta} - \boldsymbol{\theta}_{1,t} &= (\boldsymbol{I} - \boldsymbol{\kappa})(\boldsymbol{\theta} - \boldsymbol{\theta}_{2,t-1}) \\ &= (\boldsymbol{I} - \boldsymbol{\kappa})(\boldsymbol{\theta} - \boldsymbol{\theta}_{1,t}) + (\boldsymbol{I} - \boldsymbol{\kappa})(\boldsymbol{\theta}_{1,t} - \boldsymbol{\theta}_{2,t-1}) \\ &= (\boldsymbol{I} - \boldsymbol{\kappa})(\boldsymbol{\theta} - \boldsymbol{\theta}_{1,t}) + (\boldsymbol{I} - \boldsymbol{\kappa})(\boldsymbol{\theta}_{1,t} - \boldsymbol{\theta}^t_{1,t-1}) + (\boldsymbol{I} - \boldsymbol{\kappa})(\boldsymbol{\theta}^t_{1,t-1} - \boldsymbol{\theta}_{2,t-1}),\end{aligned}$$

where $\boldsymbol{\theta}^t_{1,t-1} = [F_{1,t-1}\mu_{t-1} \quad \rho F_{1,t-1}x_{t-1}]'$.

At the consensus level, the forecast error and the consensus forecast revision are given by:

$$y_t - F_t y_t = \boldsymbol{I}(\boldsymbol{\theta} - \boldsymbol{\theta}_{1,t}) \quad \text{and} \quad F_t y_t - F_{t-1} y_t = \boldsymbol{I}(\boldsymbol{\theta}_{1,t} - \boldsymbol{\theta}^t_{1,t-1}).$$

Rearrange the terms, we can get:

$$y_t - F_t y_t = \boldsymbol{I}\boldsymbol{\kappa}^{-1}(\boldsymbol{I} - \boldsymbol{\kappa})\boldsymbol{I}'(F_t y_t - F_{t-1} y_t) - \boldsymbol{I}\boldsymbol{\kappa}^{-1}(\boldsymbol{I} - \boldsymbol{\kappa})\boldsymbol{I}'(F_{2,t-1} y_t - F_{t-1} y_t),$$

which is Equation (19) in the main text. The estimated coefficient β^{Trend}_{CG} therefore is given by:

$$\begin{aligned}\beta^{Trend}_{CG} &= \frac{cov(F_t y_t - F_{t-1} y_t, y_t - F_t y_t)}{var(F_t y_t - F_{t-1} y_t)} \\ &= \frac{cov(F_t y_t - F_{t-1} y_t, \boldsymbol{I}\boldsymbol{\kappa}^{-1}(\boldsymbol{I} - \boldsymbol{\kappa})\boldsymbol{I}'(F_t y_t - F_{t-1} y_t))}{var(F_t y_t - F_{t-1} y_t)} \\ &- \frac{cov(F_t y_t - F_{t-1} y_t, \boldsymbol{I}\boldsymbol{\kappa}^{-1}(\boldsymbol{I} - \boldsymbol{\kappa})\boldsymbol{I}'(F_{2,t-1} y_t - F_{t-1} y_t))}{var(F_t y_t - F_{t-1} y_t)} \\ &= \boldsymbol{I}\boldsymbol{\kappa}^{-1}(\boldsymbol{I} - \boldsymbol{\kappa})\boldsymbol{I}' - \boldsymbol{I}\boldsymbol{\kappa}^{-1}(\boldsymbol{I} - \boldsymbol{\kappa})\boldsymbol{I}' \frac{cov(F_t y_t - F_{t-1} y_t, F_{2,t-1} y_t - F_{t-1} y_t)}{var(F_t y_t - F_{t-1} y_t)} \\ &= \frac{1 - \boldsymbol{\kappa}_{11}}{\boldsymbol{\kappa}_{11}} + \frac{1 - \boldsymbol{\kappa}_{22}}{\boldsymbol{\kappa}_{22}} + \frac{\boldsymbol{\kappa}_{11}\boldsymbol{\kappa}_{12}(\boldsymbol{\kappa}_{21} - \boldsymbol{\kappa}_{22}) + \boldsymbol{\kappa}_{22}\boldsymbol{\kappa}_{21}(\boldsymbol{\kappa}_{12} - \boldsymbol{\kappa}_{11})}{\boldsymbol{\kappa}_{11}\boldsymbol{\kappa}_{22}(\boldsymbol{\kappa}_{11}\boldsymbol{\kappa}_{22} - \boldsymbol{\kappa}_{12}\boldsymbol{\kappa}_{21})} \\ &- \boldsymbol{I}\boldsymbol{\kappa}^{-1}(\boldsymbol{I} - \boldsymbol{\kappa})\boldsymbol{I}' \frac{cov(F_t y_t - F_{t-1} y_t, F_{2,t-1} y_t - F_{t-1} y_t)}{var(F_t y_t - F_{t-1} y_t)},\end{aligned}$$

which is Equation (18) in the main text.

From the third equality, we observe that to show $\beta^{Trend}_{CG} > 0$, it is sufficient and necessary to show:

$$\frac{cov(F_t y_t - F_{t-1} y_t, F_{2,t-1} y_t - F_{t-1} y_t)}{var(F_t y_t - F_{t-1} y_t)} < 1.$$

The condition can then be rewritten as:

$$\begin{aligned}
&var(F_t y_t - F_{t-1} y_t) - cov(F_t y_t - F_{t-1} y_t, F_{2,t-1} y_t - F_{t-1} y_t) \\
&= cov(F_t y_t - F_{t-1} y_t, F_t y_t - F_{2,t-1} y_t) \\
&= \frac{1}{\Omega^2}\{[V + \sigma_e^2\sigma_\mu^2 + (1-\rho)\sigma_e^2\sigma_z^2]^2\sigma_\mu^2 + [V + \sigma_\epsilon^2\sigma_x^2 + \rho(\rho-1)\sigma_\epsilon^2\sigma_z^2]^2\sigma_x^2 \\
&+ [\sigma_\epsilon^2(\sigma_x^2 + \sigma_e^2) - \rho\sigma_e^2(\sigma_\mu^2 + \sigma_\epsilon^2)]^2\overline{\sigma}_z^2\} \\
&> 0,
\end{aligned}$$

where $\overline{\sigma}_z^2 = E[(\overline{E}[z_{i,t}])^2]$ is the variance of separation error at the consensus level.

The intuition follows from the first equality. Note that the term $F_t y_t - F_{t-1} y_t$ represents the revision in forecast between the current period and the previous period after observing the private signal. The term $F_t y_t - F_{2,t-1} y_t$ represents the revision in forecast between the current period and the forecast at the end of the previous period after observing the actual state y_{t-1}. Therefore, their covariance shall be positive.

Proof of Proposition 5. To simplify the notation, we define:

$$FE_{i,t}^{\mu} = \mu_t - \mu_{1,t}^i; \quad FE_{i,t}^{x} = x_t - x_{1,t}^i.$$

Then, the forecast error regarding h periods ahead could be written as:

$$FE_{i,t}^{h} = FE_{i,t}^{\mu} + \rho^h FE_{i,t}^{x} + ER^h,$$

where $ER^h = \sum_{j=1}^{h} \gamma_{t+j}^{\mu} + \rho^j \gamma_{t+j}^{x}$ contains the state innovations from period $t+1$ to $t+h$, which are orthogonal to the forecast revision.

Similarly, the forecast revision regarding h periods ahead could be rewritten as:

$$\begin{aligned}
FR_{i,t}^{h} &= FR_{i,t}^{\mu} + \rho^h FR_{i,t}^{x} \\
&= (-FE_{i,t}^{\mu} + FE_{i,t-1}^{\mu} + \gamma_t^{\mu}) + \rho^h(-FE_{i,t}^{x} + \rho FE_{i,t}^{x} + \gamma_t^{x}),
\end{aligned}$$

where $FR_{i,t}^{\mu}$ and $FR_{i,t}^{x}$ denote the belief revision regarding the trend and cyclical components.

Then the covariance between the forecast error and forecast revision could be written as:

$$\mathrm{Cov}(FE_{i,t}^{h}, FR_{i,t}^{h}) = \mathrm{Cov}(FE_{i,t}^{\mu}, FR_{i,t}^{\mu}) + \rho^h \mathrm{Cov}(FE_{i,t}^{x}, FR_{i,t}^{\mu}) + \rho^h \mathrm{Cov}(FE_{i,t}^{\mu}, FR_{i,t}^{x}) + \rho^{2h} \mathrm{Cov}(FE_{i,t}^{x}, FR_{i,t}^{x}). \tag{B18}$$

The variance of the forecast revision is:

$$\text{Var}(FR^h_{i,t}) = \text{Var}(FR^\mu_{i,t}) + \rho^{2h}\text{Var}(FR^x_{i,t}) + 2\rho^h\text{Cov}(FR^\mu_{i,t}, FR^x_{i,t}).$$

The coefficients for the short-run ($h = 0$) and long-run ($h = \infty$) are:

$$\beta^0 = \frac{\text{Cov}(FE^\mu_{i,t}, FR^\mu_{i,t}) + \text{Cov}(FE^x_{i,t}, FR^\mu_{i,t}) + \text{Cov}(FE^\mu_{i,t}, FR^x_{i,t}) + \text{Cov}(FE^x_{i,t}, FR^x_{i,t})}{\text{Var}(FR^\mu_{i,t}) + \text{Var}(FR^x_{i,t}) + 2\text{Cov}(FR^\mu_{i,t}, FR^x_{i,t})};$$

and

$$\beta^\infty = \frac{\text{Cov}(FE^\mu_{i,t}, FR^\mu_{i,t})}{\text{Var}(FR^\mu_{i,t})}.$$

We then consider the case when forecasters are overconfident in the trend signal, i.e., $m < 1$. The posterior beliefs regarding the two components after observing the new signals can be written as:

$$\mu^T_{1,t,o} = \frac{m\sigma^2_\epsilon(\rho^2\sigma^2_{z,o} + \sigma^2_x + \sigma^2_e)}{\Omega_1}\mu^i_{2,t-1,o} + \frac{V_1 + \sigma^2_e(\sigma^2_{z,o} + \sigma^2_\mu)}{\Omega_1}s^\mu_{i,t} - \frac{\rho m\sigma^2_\epsilon\sigma^2_{z,o}}{\Omega_1}(s^x_{i,t} - \rho x^i_{2,t-1,o}),$$

$$x^T_{1,t,o} = \frac{\sigma^2_e(\sigma^2_{z,o} + \sigma^2_\mu + m\sigma^2_\epsilon)}{\Omega_1}\rho x^i_{2,t-1,o} + \frac{V_1 + m\sigma^2_\epsilon(\sigma^2_x + \rho^2\sigma^2_{z,o})}{\Omega_1}s^x_{i,t} - \frac{\rho\sigma^2_e\sigma^2_{z,o}}{\Omega_1}(s^\mu_{i,t} - \mu^i_{2,t-1,o}),$$

where Ω_1 and V_1 are constants:

$$\Omega_1 = (\sigma^2_{z,o} + \sigma^2_\mu + m\sigma^2_\epsilon)(\sigma^2_x + \sigma^2_e + \rho^2\sigma^2_{z,o}) - \rho^2\sigma^4_{z,o},\ V_1 = (\sigma^2_{z,o} + \sigma^2_\mu)(\sigma^2_x + \rho^2\sigma^2_{z,o}) - \rho^2\sigma^4_{z,o}.$$

The term $\sigma^2_{z,o}$ is the perceived variance of the separation error in the steady state in this case. The variance-covariance matrix regarding the beliefs of the trend and cyclical components is:

$$\begin{pmatrix} \text{Var}^T_o & \widetilde{\text{COV}}_o \\ \widetilde{\text{COV}}_o & \text{Var}^C_o \end{pmatrix} = \begin{pmatrix} \frac{m\sigma^2_\epsilon[\Omega_1 - m\sigma^2_\epsilon(\sigma^2_x + \sigma^2_e + \rho^2\sigma^2_{z,o})]}{\Omega_1} & -\frac{\rho\sigma^2_e m\sigma^2_\epsilon\sigma^2_{z,o}}{\Omega_1} \\ -\frac{\rho\sigma^2_e m\sigma^2_\epsilon\sigma^2_{z,o}}{\Omega_1} & \frac{\sigma^2_e[\Omega_1 - \sigma^2_e(m\sigma^2_\epsilon + \sigma^2_\mu + \sigma^2_{z,o})]}{\Omega_1} \end{pmatrix}.$$

Note that when forecasters are rational, i.e., $m = 1$, all the terms in Equation (B18) are zero. When forecasters are overconfident in the trend signal, the terms are given by:

$$\text{Cov}(FE^\mu_{i,t'}, FR^\mu_{i,t}) = -\lambda^T + \frac{-m_1\sigma^2_\epsilon(\sigma^2_e + \sigma^2_x)}{\Omega_1(\text{Var}^T_o + \text{Var}^C_o + 2\widetilde{\text{COV}}_o))}[(\text{Var}^C_o + \widetilde{\text{COV}}_o) * \lambda^T - (\text{Var}^T_o + \widetilde{\text{COV}}_o) * \lambda^{cov}];$$

$$\text{Cov}(FE^x_{i,t}, FR^\mu_{i,t}) = -\lambda^{cov} + \frac{-m_1\rho\sigma_\epsilon^2(\sigma_e^2+\sigma_x^2)}{\Omega_1(\text{Var}_o^T + \text{Var}_o^C + 2\widetilde{\text{COV}}_o))}[(\text{Var}_o^C + \widetilde{\text{COV}}_o) * \lambda^{cov} - (\text{Var}_o^T + \widetilde{\text{COV}}_o) * \lambda^C];$$

$$\text{Cov}(FE^\mu_{i,t}, FR^x_{i,t}) = -\lambda^{cov} - \frac{-\rho\sigma_e^2(\sigma_\mu^2+m_1\sigma_\epsilon^2)}{\Omega_1(\text{Var}_o^T + \text{Var}_o^C + 2\widetilde{\text{COV}}_o))}[(\text{Var}_o^C + \widetilde{\text{COV}}_o) * \lambda^T - (\text{Var}_o^T + \widetilde{\text{COV}}_o) * \lambda^{cov}];$$

$$\text{Cov}(FE^x_{i,t}, FR^x_{i,t}) = -\lambda^C - \frac{-\rho^2\sigma_e^2(\sigma_\mu^2+m_1\sigma_\epsilon^2)}{\Omega_1(\text{Var}_o^T + \text{Var}_o^C + 2\widetilde{\text{COV}}_o))}[(\text{Var}_o^C + \widetilde{\text{COV}}_o) * \lambda^{cov} - (\text{Var}_o^T + \widetilde{\text{COV}}_o) * \lambda^C],$$

where $\lambda^T > 0$, $\lambda^C > 0$ and $\lambda^{cov} < 0$ are the difference between the objective belief and the actual ones:

$$\begin{aligned}
\lambda^T &= \text{Var}_a^T - \text{Var}_o^T \\
&= (1-m)\sigma_\epsilon^2(\frac{V_1+\sigma_e^2(\sigma_{z,o}^2+\sigma_\mu^2)}{\Omega_1})^2 + (\frac{m\sigma_\epsilon^2(\sigma_x^2+\sigma_e^2)}{\Omega_1})^2(\sigma_{z,a}^2-\sigma_{z,o}^2); \\
\lambda^C &= \text{Var}_a^C - \text{Var}_o^C \\
&= (1-m)\sigma_\epsilon^2(\frac{\rho\sigma_e^2\sigma_{z,o}^2}{\Omega_1})^2 + (\frac{\rho\sigma_e^2(\sigma_\mu^2+m\sigma_\epsilon^2)}{\Omega_1})^2(\sigma_{z,a}^2-\sigma_{z,o}^2); \\
\lambda^{cov} &= \widetilde{\text{COV}}_a - \widetilde{\text{COV}}_o \\
&= -(1-m)\sigma_\epsilon^2\frac{\rho\sigma_e^2\sigma_{z,o}^2}{\Omega_o}\frac{V_1+\sigma_e^2(\sigma_{z,o}^2+\sigma_\mu^2)}{\Omega_1} - \frac{m\sigma_\epsilon^2(\sigma_x^2+\sigma_e^2)}{\Omega_1}\frac{\rho\sigma_e^2(\sigma_\mu^2+m\sigma_\epsilon^2)}{\Omega_1}(\sigma_{z,a}^2-\sigma_{z,o}^2).
\end{aligned}$$

The subscript a stands for the actual variance and covariance term when forecasters are overconfident in the trend signal. $\sigma_{z,a}^2$ is the actual variance of the separation error:

$$\sigma_{z,a}^2 - \sigma_{z,o}^2 = G^T(1-m)\sigma_\epsilon^2(\frac{\sigma_e^2 V_1}{\Omega_1})^2 > 0,$$

where G^T is given by:

$$G^T = \frac{\Omega_1^2}{[\Omega_1(\text{Var}_1^T + \text{Var}_1^C + 2\widetilde{\text{COV}}_1)]^2 - [m\sigma_e^2\sigma_\epsilon^2(\rho\sigma_\mu^2+\sigma_x^2)]^2} > 0.$$

We only focus the case when the extent of overconfident is sufficiently large, i.e., $m_1 \to 0$. In this case:

$$\text{Cov}(FE^\mu_{i,t}, FR^\mu_{i,t}) = -\sigma_\epsilon^2; \quad \text{Cov}(FE^x_{i,t}, FR^\mu_{i,t}) = 0;$$

$$\text{Cov}(FE^{\mu}_{i,t}, FR^{x}_{i,t}) = -\frac{\rho\sigma_e^2\sigma_\epsilon^2}{\sigma_e^2+\sigma_x^2}; \quad \text{Cov}(FE^{x}_{i,t}, FR^{x}_{i,t}) = -\frac{\rho^2\sigma_e^2\sigma_\epsilon^2}{(\sigma_e^2+\sigma_x^2)^2}.$$

The difference between the coefficients of short-run and long-run then is given by:

$$\beta^L - \beta^S = const * \sigma_\epsilon^2\sigma_e^2\sigma_x^2 * \underbrace{\{\rho\sigma_e^2\sigma_\mu^2(\rho\sigma_e^2+\sigma_e^2+\sigma_x^2) - \sigma_e^2(\rho^2-1)[\rho^2\sigma_e^2\sigma_\epsilon^2+\sigma_x^2(\sigma_e^2+\sigma_x^2)] - \sigma_x^2(\sigma_e^2+\sigma_x^2)^2\}}_{\kappa^T},$$

where $const = \frac{1}{\text{Var}_o^T + \text{Var}_o^C + 2\widetilde{\text{COV}}_o} > 0$.

In the following, we show that κ^T cross zero once from above. First, when $\sigma_x^2 = 0$, we have: $\kappa^T = \rho\sigma_e^4[\rho(1-\rho^2)\sigma_\epsilon^2 + (1+\rho)\sigma_\mu^2] > 0$. Second, when σ_x^2 is sufficiently large, $\kappa^T < 0$. Third, we derive its derivative with respect to σ_x^2:

$$\frac{\kappa^T}{\partial\sigma_x^2} = \rho\sigma_e^2\sigma_\mu^2 + (1-\rho^2)\sigma_e^2(\sigma_e^2+2\sigma_x^2) - 2\sigma_x^2(\sigma_e^2+\sigma_x^2) - (\sigma_e^2+\sigma_x^2)^2.$$

This derivative monotonically decreases in σ_x^2. In addition, it is positive when $\sigma_x^2 = 0$ and negative when σ_x^2 is large enough. Therefore it crosses zero from above only once. Finally, given these three properties, κ^T crosses zero from above only once.

Therefore, there exists a unique cutoff σ_x^* such that $\beta^L < \beta^S < 0$ if and only if $\sigma_x > \sigma_x^*$, which establishes the proposition.

B.2 Supplemental Material for Section 4.4

Special case when the trend component is observable. Consider a special case where both the state and trend components are observable at the end of each period. Without loss of generality, we assume the cyclical component follows an AR(N) process:

$$x_t = \sum_{h=0}^{N} \rho^h L^h x_t + \gamma_t^x,$$

where L is the lag operator.

The private signal of forecaster i is given by:

$$s^{\mu}_{i,t} = \mu_t + \epsilon_{i,t} \quad \text{and} \quad s^{x}_{i,t} = x_t + e_{i,t}.$$

Given the trend component is observable at the end of each period, one's prior belief before observing the signals is:

$$\boldsymbol{\theta}^i_{2,t-1} = \begin{pmatrix} \mu_{t-1} \\ \sum_{h=0}^{N} \rho^h L^h x_t \end{pmatrix}.$$

The posterior beliefs regarding the two components upon observing the signals is given by:

$$\boldsymbol{\theta}^i_{1,t} = \boldsymbol{\theta}^i_{2,t-1} + \boldsymbol{\kappa} \times (\boldsymbol{s}_{i,t} - \boldsymbol{\theta}^i_{2,t-1}),$$

where the Kalman gain matrix and the variance-covariance matrix is same as the ones in the main text:

$$\boldsymbol{\kappa} = \begin{pmatrix} \frac{\sigma^2_\mu}{\sigma^2_\mu+\sigma^2_\epsilon} & 0 \\ 0 & \frac{\sigma^2_x}{\sigma^2_x+\sigma^2_e} \end{pmatrix}, \quad \text{and} \quad \begin{pmatrix} \text{Var}^T_s & \widetilde{\text{COV}}_s \\ \widetilde{\text{COV}}_s & \text{Var}^C_s \end{pmatrix} = \begin{pmatrix} \frac{\sigma^2_\epsilon\sigma^2_\mu}{\sigma^2_\epsilon+\sigma^2_\mu} & 0 \\ 0 & \frac{\sigma^2_e\sigma^2_x}{\sigma^2_x+\sigma^2_e} \end{pmatrix}.$$

The forecast dispersion across forecasters is given by:

$$\begin{aligned} E[(F_{i,t}y_{t+h} - \overline{E}[F_{i,t}y_{t+h}])^2] &= \rho^{2h} \underbrace{\frac{\sigma^2_x}{\sigma^2_x+\sigma^2_e}}_{\phi^C_s} \text{Var}^C_s + \underbrace{\frac{\sigma^2_\mu}{\sigma^2_\mu+\sigma^2_\epsilon}}_{\phi^T_s} \text{Var}^T_s \\ &= \rho^{2h}(\frac{\sigma^2_x}{\sigma^2_x+\sigma^2_e})^2\sigma^2_e + (\frac{\sigma^2_\mu}{\sigma^2_\mu+\sigma^2_\epsilon})^2\sigma^2_\epsilon. \end{aligned}$$

It is evidence that the forecast variance across forecasters is decreasing, as the forecast horizon extends.

In addition, changes in trend forecasts and changes cyclical forecasts can be written as follows:

$$F_{i,t}y_{t+3Y} - F_{i,t-1}y_{t-1+3Y} = (\mu^i_{1,t} - E_{i,t-1}[\mu_{t-1}]) + \rho^{3Y}(E_{i,t}[\sum_{h=0}^{N}\rho^h L^h x_{t+3Y}] - E_{i,t-1}[\sum_{h=0}^{N}\rho^h L^h x_{t+3Y-1}]),$$

and

$$Cyc_{i,t} - Cyc_{i,t-1} = (1-\rho^{3Y})(E_{i,t}[\sum_{h=0}^{N}\rho^h L^h x_{t+3Y}] - E_{i,t-1}[\sum_{h=0}^{N}\rho^h L^h x_{t+3Y-1}]).$$

Following the same logic as the main text, the covariance between changes in the beliefs about the trend component and changes in beliefs about the cyclical component at any horizon should be non-negative. That is,

$$\begin{aligned} &COV^h_F(F_{i,t}y_{t+3Y} - F_{i,t-1}y_{t-1+3Y}, Cyc_{i,t} - Cyc_{i,t-1}) \\ &= \rho^{3Y}(1-\rho^{3Y})Var(E_{i,t}[\sum_{h=0}^{N}\rho^h L^h x_{t+3Y}] - E_{i,t-1}[\sum_{h=0}^{N}\rho^h L^h x_{t+3Y-1}]) \geq 0. \end{aligned}$$

In this special case, where trends and cycles are observable at the end of each period, the model fails to replicate either of the two empirical patterns documented, even when we allow the data generation process for the cyclical component to follow an

AR(N) process.

Special case when the cyclical component is transitory. In the following, we provide the model prediction when the cyclical component is transitory. The forecast dispersion across forecasters in this special case is given by:

$$\text{Forecast dispersion}_{th} = E[(F_{i,t}y_{t+h} - \overline{E}[F_{i,t}y_{t+h}])^2] = \begin{cases} \phi_s^T \text{Var}^T & \text{if } h > 0 \\ \phi_s^T \text{Var}^T + \phi_s^C \text{Var}^C & \text{if } h = 0 \end{cases},$$

where ϕ_s^C, ϕ_s^T are constants that less than one, and $\overline{E}[\cdot]$ is the mean forecast across all forecasters. The model predicts that the forecast dispersion across forecasters will drop at $h = 1$, and remains constant for $h > 1$.

In this special case, the changes in the long-run and cyclical forecasts are given by:

$$F_{i,t}y_{t+3Y} - F_{i,t-1}y_{t-1+3Y} = E_{i,t}[\mu_t] - E_{i,t-1}[\mu_{t-1}],$$

and

$$Cyc_{i,t}^h - Cyc_{i,t-1}^h = \begin{cases} 0 & \text{if } h > 0 \\ E_{i,t}x_t - E_{i,t-1}x_{t-1} & \text{if } h = 0 \end{cases}.$$

Therefore, the model predicts a zero covariance between changes in the long-run forecasts and cyclical forecasts for all h.

The generalization. This following part presents the full characterization of the generalized case. The states are as follows:

$$y_t = \mu_t + x_t,$$

$$\mu_t = \rho^\mu \mu_{t-1} + \gamma_t^\mu; \quad x_t = \rho^x x_{t-1} + \gamma_t^x.$$

ρ^μ and ρ^x capture the persistence of the two components. When $\rho^\mu = 1$, we get our baseline model, and when $\rho^\mu = 0$, the model degenerate to the model where state variable follows an AR(1) process.

The information structure is the same as the baseline model. In each period, forecasters observe a private signal for each component:

$$s_{i,t}^\mu = \mu_t + \epsilon_{i,t}; \quad s_{i,t}^x = x_t + e_{i,t}.$$

Belief Updating In this scenario, forecasters posterior belief $\boldsymbol{\theta}_{1,t}^i = (\mu_{1,t}^i, x_{1,t}^i)'$ upon observing private signal is given by:

$$\mu_{1,t}^i = \frac{\rho_\mu \sigma_\epsilon^2(\rho_x^2 \sigma_{z,t-1}^2 + \sigma_x^2 + \sigma_e^2)}{\Omega^G}\mu_{2,t-1}^i + \frac{V^G + \sigma_e^2(\rho_\mu^2 \sigma_z^2 + \sigma_\mu^2)}{\Omega^G}s_{i,t}^\mu - \frac{\rho_\mu \rho_x \sigma_\epsilon^2 \sigma_z^2}{\Omega^G}(s_{i,t}^x - \rho x_{2,t-1}^i), \tag{B19}$$

$$x^i_{1,t} = \frac{\sigma^2_e(\rho^2_\mu\sigma^2_z + \sigma^2_\mu + \sigma^2_\epsilon)}{\Omega^G}\rho x^i_{2,t-1} + \frac{V^G + \sigma^2_\epsilon(\sigma^2_x + \rho^2_x\sigma^2_z)}{\Omega^G}s^x_{i,t} - \frac{\rho_\mu\rho_x\sigma^2_e\sigma^2_z}{\Omega^G}(s^\mu_{i,t} - \mu^i_{2,t-1}), \tag{B20}$$

where Ω^G and V^G are constants:

$$\Omega^G = (\sigma^2_\epsilon + \sigma^2_\mu + \rho^2_\mu\sigma^2_z)(\rho^2_x\sigma^2_z + \sigma^2_e + \sigma^2_x) - \rho^2_x\rho^2_\mu\sigma^2_z,$$

$$V^G = (\rho^2_\mu\sigma^2_z + \sigma^2_\mu)(\sigma^2_x + \rho^2_x\sigma^2_z) - \rho^2_\mu\rho^2_x\sigma^4_z.$$

And the variance-covariance matrix becomes:

$$\begin{pmatrix} \text{Var}^T_G & \widetilde{\text{COV}}_G \\ \widetilde{\text{COV}}_G & \text{Var}^C_G \end{pmatrix} = \begin{pmatrix} \frac{\sigma^2_\epsilon[\Omega^G - \sigma^2_\epsilon(\sigma^2_x + \sigma^2_e + \rho^2_x\sigma^2_z)]}{\Omega^G} & -\frac{\rho_\mu\rho_x\sigma^2_e\sigma^2_\epsilon\sigma^2_z}{\Omega^G} \\ -\frac{\rho_\mu\rho_x\sigma^2_e\sigma^2_\epsilon\sigma^2_z}{\Omega^G} & \frac{\sigma^2_e[\Omega^G - \sigma^2_e(\sigma^2_\epsilon + \sigma^2_\mu + \rho^2_\mu\sigma^2_z)]}{\Omega^G} \end{pmatrix}. \tag{B21}$$

As in the baseline model, σ^2_z has a unique steady state:

$$\sigma^2_z = \frac{-\{\sigma^2_e\sigma^2_\epsilon[(1-\rho^2_m)\sigma^2_x + (1-\rho^2_x)\sigma^2_\mu] + \sigma^2_\mu\sigma^2_x(\sigma^2_e + \sigma^2_\epsilon)\} + \Lambda^G}{2[\sigma^2_e\sigma^2_\epsilon(\rho_m - \rho_x)^2 + (\sigma^2_e + \sigma^2_\epsilon)(\rho^2_m\sigma^2_x + \rho^2_x\sigma^2_\mu)]}, \tag{B22}$$

where

$$\Lambda^G = \sqrt{2\sigma^2_e\sigma^2_\epsilon\sigma^2_\mu\sigma^2_x[\sigma^2_e\sigma^2_\epsilon(\rho_m - \rho_x)^2 + (\sigma^2_e + \sigma^2_\epsilon)(\rho^2_m\sigma^2_x + \rho^2_x\sigma^2_\mu)] + \sigma^4_e\sigma^4_\epsilon[(\rho^2_m\sigma^2_x + \rho^2_x\sigma^2_\mu)^2 - 2(\rho_m\sigma^2_x + \rho_x\sigma^2_\mu)]}.$$

B.3 Common Shock

In this section, we analyze the case of correlated trend and cyclical components driven by a common shock, by following Delle Monache et al. (2024). They show the presence of a common shock influencing both the trend and cyclical components of GDP growth in the same direction.

This common shock assumption is widely used in the literature. It captures situations where economic shocks have both transitory and permanent effects. Many studies show that recessions impact the economy in both temporary and lasting ways. For example, Furlanetto et al. (2025) and Antolin-Diaz et al. (2017) show that supply shocks can negatively affect both the cyclical and permanent components of GDP. Similarly, Almeida et al. (2004) finds that an increase in firms' profitability can permanently elevate their cash flows while also boosting short-term cash flows by reducing potential losses.

In this section, we consider the following state generation process:

$$y_t = \mu_t + x_t,$$

$$\mu_t = \mu_{t-1} + \gamma_t^{\mu} + \delta_t \quad \text{and} \quad x_t = \rho x_{t-1} + \gamma_t^{x} + b\delta_t,$$

where δ_t is a common shock affecting both the trend and cyclical components. This shock is normally distributed with zero mean and variance σ_δ^2, and is independent across periods (i.e., $\delta_t \sim N(0, \sigma_\delta^2)$). The scalar b measures the relative importance of the shock to each of these components. Notably, following Delle Monache et al. (2024), we assume that b is positive, thereby capturing the common shock assumption.

To contrast with our benchmark model, we assume in this case that the trend component becomes observable at the end of each period. With the information structure, the belief updating process is given by:

$$\boldsymbol{\theta}_{1,t}^i = \boldsymbol{\theta}_{2,t-1}^i + \boldsymbol{\kappa}_{cor}(\boldsymbol{s}_{i,t} - \boldsymbol{\theta}_{2,t-1}^i), \tag{B23}$$

where $\boldsymbol{\theta}_{2,t-1}^i = (\mu_{t-1}, \rho x_{t-1})'$. Since forecasters are able to observe the actual trend and cyclical components at the end of each period, $\boldsymbol{\kappa}_{cor}$ is the corresponding Kalman gain matrix given by:

$$\boldsymbol{\kappa}_{cor} = \begin{pmatrix} \frac{\tau_2^{\mu}}{\tau_1^{\mu}+\tau_2^{\mu}+\tau_3^{\mu}} & \frac{\tau_3^{\mu}}{b(\tau_1^{\mu}+\tau_2^{\mu}+\tau_3^{\mu})} \\ \frac{b\tau_3^{x}}{\tau_1^{x}+\tau_2^{x}+\tau_3^{x}} & \frac{\tau_2^{x}}{\tau_1^{x}+\tau_2^{x}+\tau_3^{x}} \end{pmatrix}, \tag{B24}$$

where $\tau_1^{\mu}, \tau_2^{\mu}, \tau_3^{\mu}, \tau_1^{x}, \tau_2^{x}, \tau_3^{x}$ are the precisions of information:

$$\tau_1^{\mu} = \frac{1}{\sigma_\mu^2 + \sigma_\delta^2}; \quad \tau_2^{\mu} = \frac{1}{\sigma_\epsilon^2}; \quad \tau_3^{\mu} = \frac{b^2}{b^2\sigma_\mu^2 + \sigma_x^2 + \sigma_e^2};$$

$$\tau_1^{x} = \frac{1}{\sigma_x^2 + b^2\sigma_\delta^2}; \quad \tau_2^{x} = \frac{1}{\sigma_e^2}; \quad \tau_3^{x} = \frac{1}{b^2\sigma_\mu^2 + b^2\sigma_\epsilon^2 + \sigma_x^2}.$$

As shown in Equation (B24), the elements on the sub-diagonal is non-zero if $b \neq 0$. Given $b > 0$, the sub-diagonal elements are positive. This is because the surprise from the trend signal (i.e., $s_{i,t}^{\mu} - \mu_{t-1}$) contains information about the common shock, which also affects the cyclical components. Therefore, forecasters would use the trend signal to update their belief about the cyclical belief, and vice versa.

We show that in this case, the covariance between forecasters' trend beliefs and cyclical beliefs (i.e., $\widetilde{\text{COV}}_{cor}$) is always positive:

$$\widetilde{\text{COV}}_{cor} \propto b(\sigma_\delta^2 + \sigma_\mu^2)[b^2(\sigma_\epsilon^2 + \sigma_\mu^2) + \sigma_e^2 + \sigma_x^2][\sigma_\delta^2(b^2\sigma_\epsilon^2 + b^2\sigma_\mu^2 + \sigma_e^2 + \sigma_x^2) + \sigma_e^2(\sigma_\epsilon^2 + \sigma_\mu^2) + \sigma_\epsilon^2\sigma_x^2]. \tag{B25}$$

With a positive covariance, predictions of this particular case would be similar to

the special case discussed in Section 4.4, and therefore inconsistent with the observed empirical pattern.